Report on Conceptual Design of CFETR Tokamak Machine v1.1

Abstract

This is a technical document which describes the conceptual design of the CFETR main components, including the TF, PF and CS magnets, the Vacuum Vessel, the Thermal Shield and Cryostat.

CFETR is a test tokamak reactor which is built by theNational Integration Design Group for Magnetic Confinement Fusion Reactor, the partner list includes the University of Science and Technology of China (USTC), the Institute of Plasma Physics, Chinese Academy of Science (ASIPP),and the Southwestern Institute of Physics (SWIP).

Contents

Figure contents

Table contents

1 Overview

The scheme is based on “The Estimating Parameters for CFETR” from Mr Wan BaoNian. To realize the requirement of TBR ≧ 1.2, enough space for tritium breeding（about0.8 - 1.0 m）need to be arranged, and the design experience of EAST, ITER and the muti-function reactor of ASIPP can be taken.

1.1 Foundation of the concept design

Major radius of plasma： R = 5.5 m

Minor radius of plasma： a = 1.6 m

Center field： Bt = 4.5/5.3 T

Enlongation： κ = 1.8

Triangularity： δ = 0.4

Thickness of blanket： about 0.8 - 1.0 m

1.2 Basic outline of the Vacuum Vessel structure

The philosophy for the VV structure design is to save the space for VV as much as possible. According to the basic dimension of the structure: R=5.5m,a=1.6m, Enlongation=1.8 and Triangularity=0.4, we get the X point coordinate (4860,2880). The detailed specification is showed as follow:

To meet the requirement of baking, cooling and neutron shielding, the vacuum vessel is designed as a double-walled structure made of nonmagnetic stainless steel. The inner and outer shells and stiffening ribs between them are joined by welding. To reduce the difficulty of manufacturing, the cross-section of the VV (D-shape) is made up of five arcs and one straight line which are tangent to each other. To simplify and optimize the processing and manufacturing, the same center point is set for VV inner shell, VV outer

shell, VVTS and TF orthodrome. According to the design experience of EAST and ITER, the two shells are both scheduled for 50mm in thickness. Considering the different influence of the neutron irradiation dose to the superconducting magnet unequal thickness of double-walled structure at inboard and outboard regions is adopt. A space of 180mm is reserved for in-wall shielding (IWS) structure , baking and cooling systems for the inboard area at the equatorial plane, as well as 400mm for the outboard area. The dimensions will be finally determined according to the results of the blanket neutron shielding analysis after the blanket concept design is completed. From VV inner shell to the boundary of the plasma, a space wider than 1000mm is reserved to arrange the tritium breeding blanket, divertor, inner coils with their supports and the cooling system etc. The maximum size inside the vacuum vessel is about 5205mm at the horizontal direction , and 8880mm at the vertical direction .

1.3 Basic outline of the VV thermal shield

Considering the requirement of the pipeline and support of VV thermal shield plate structure, the basic dimension of VV thermal shielding (inner thermal shielding) is set to 50mm. Similar to VV, VVTS structure is comprised of five arcs and one straight line which are tangent to each other. For the convenience of manufacture and installation, the center point of VVTS' orthodrome is designed to be the same as VV's at the horizontal plane. For this integrated design of VVTS and TF magnet, the physics interval between them is set to 50mm, considering the design of VVTS' support is based on that of TF magnet. For VVTS is basically supported by TF magnet, its basic outline is consistent with TF. Considering the contraction of the magnet in cooling and the expansion of VV in baking, the intervals between VV and VVTS at inboard and outboard region are respectively scheduled for 50mm and 200mm at the center plane.

1.4 Basic outline of the Toroidal Field magnet

18 toroidal field magnets are adopted for preliminary consideration. To guarantee central field high enough, sufficient space for the cross-section of toroidalfield(TF) coil winding should be reserved, and a radial dimension of 750 mm is reserved. It is estimated that conductor designed for 60-70 kA could meet the total ampere turns current of coil winding, which is about 7800 kA to 9100 kA. (The total nominal current of ITER toroidal field coil winding is 9112 kA). The D-shaped cross-section of toroidal field magnet is composed of five arcs and one straight line which are tangent to each other. The length for one double-pancake winding is about 700mm. The space between TF magnet and VVTS is scheduled for 50mm for heat and electric insulation demand. There is 100 mm reserved inside TF magnet for the centripetal-force-resisting support and toroidal support structure. A thickness of 40 mm is reserved for lateral plate of TF magnet, as well as about 43 to 73 mm for inside support plate. The dimension of winding cross section is about 536 mm × 618 mm. The D-shaped cross-section of TF magnet has yet to be optimized by Princeton-D pure tension coil theory. At present, the height and width of TF magnet is about 12m and 8m respectively.

1.5 Basic outline of the Central Solenoid magnet

The radial space of solenoid is scheduled for 490 mm. To guarantee the necessary magnetic flux, the inner and outer diameter of central solenoid is scheduled for 2300mm and 3280mm respectively. The final dimension will be determined according to the results of the detailed analysis .

1.6 Further research work

- Given the distribution of 18 TF magnets and that the total current is about 7800 kA to 9100 kA, the magnetic field at the plasma centre point (5.5m,0)

need to be calculated. And necessary adjustment is to be done.

- Given the distribution of TF magnets widing and 60-70 kA turn current, the peak magnetic field and its position are to be estimated.
- The D-shaped cross-section of TF magnet has yet to be optimized by Princeton-D pure tension coil theory.
- The design of VV need to be optimized according to the structure requirements of the tritium breeding blanket and divertor.
- The volt-second and maximum field provided by CS need to be estimated. And necessary adjustment is to be done.
- The physics group can carry out preliminary simulation by the present design and do necessary optimization and adjustments according to the simulation results.

The Figure 1 and Figure 2show the outline and size distribution of the major components of Tokamak machine.

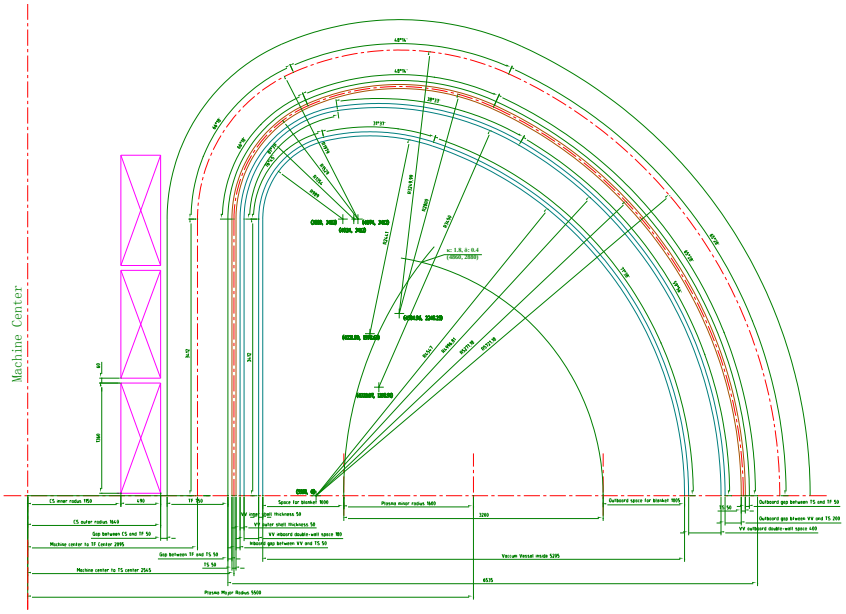

Figure 1 layout of the main components

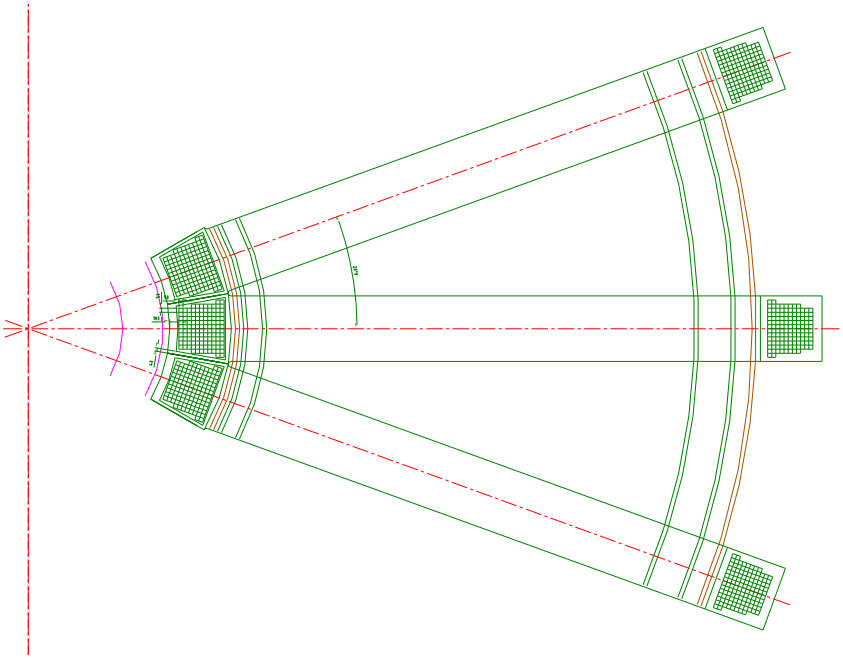

Figure 2 top view of the main components

2 TF coil

2.1 System description

2.1.1 Basic functions

·The toroidal field coil system provides a toroidal field with a 1/R variation of magnitude, with a value of up to 4.5T at a radius of 5.5 m.

·The toroidal field coil system has 18 coils.

·All coils shall be de-energised during Glow Discharge cleaning. The coils shall be available for use during other vessel cleaning operations.

·All coils shall be de-energised during vacuum vessel dust-removal operations, as long as there are not more than 200 such de-energisation cycles.

·The magnet system allows access to the vacuum vessel and plasma between the toroidal and poloidal coil set in the divertor, equatorial and upper port levels. These gaps are restricted to the extent necessary to provide inter-coil support between the toroidal coils.

·The magnets may be used to provide local support to the thermal shield.

2.1.2 Basic configurations

·The shape of the TF coil perimeter has been reach by a process of iteration. The conventional lowest in-plane stress TF coil shape is well-known “bending moment free D”.

·The contour of the D-shaped coil consists of five arcs and a straight leg. The straight leg of the coil with wedge is squeezed each other to form an inner arch. The adjacent inter-coil structure is of wedge-shaped across-section. External wedge chocks of the

torus are also squeezed each other with coil to form an outer arch. Two arches resist strong centering force and overturning torque.

·The magnet system consists of: Toroidal field (TF) coils, and associated structures, including gravity supports and precompression rings

2.2 System design requirements

2.2.1 System specific requirements

·Coils shall not quench during plasma operation, including plasma disruptions.

·The coil quench detection system must be able to distinguish between electromagnetic and thermal disturbances caused by normal operation and a superconductor quench.

·During a fast discharge of the TF coils, a low temperature quench may occur, resulting in He expulsion from the coils.

·The target accuracy of detection for 'false quench' events within the TF coil system is less than1 per year.

·The superconducting bus-bars shall be capable of full current operation (greater than 1 minute) without causing any damage, even if quenched and un-cooled.

·Although adding complexity in the form of a cryostat, the TF magnetic system can then operate at a constant temperature and take advantage of the high strength of cryogenic steel (namely 316LN), allowing simplification and a size reduction of the support structure.

2.2.2 Mechanical requirements (including load conditions)

The magnets shall withstand the following:

·Electromagnetic loads

Electromagnetic forces induced on in-vessel components and transmitted to the

magnets

·Gravity and seismic loads on the magnets and those transmitted from any parts of the thermal shield supported on them

·Thermal stresses during cooldown and warm-up

·Precompression loads applied during assembly

·Helium coolant pressure loads

·Thermal elongation loads due to differential contraction between the magnets and the cryostat wall (mainly on the feeders).

2.2.3 External operational requirements on the magnets

There are a set of external operational requirements on the magnets that have been reach after consideration of the overall machine design:

·All of magnets (include TF, PF and CS) must be capable of providing a long pulse capability.

·The TF magnet system should be capable of continuing normal operated in the event of plasma disruptions (i.e. a disruption should not cause a magnet quench).

·The TF magnet system must be designed, built and operated so that credible magnet system failures, which could occur under normal and abnormal condition (including the specified safety earthquake), cannot cause damage to the total CFETR device system.

·The TF magnet system consists of 18 TF coils, and the design of TF system will permit plasma operation with the toroidal field in either direction.

2.3 Conceptual Design Description

2.3.1 The scheme of the main components of CFETR

The scheme is based on “The Estimating Parameters for CFETR” from Wan BaoNian.

To realize the requirement of TBR ≧ 1.2, enough space for tritium breeding（about0.8 - 1.0 m）need to be arranged, and the design experience of EAST, ITER and the muti-function reactor of ASIPP can be taken. The scheme only refers to the basic design of the outline and dimensions for Vacuum Vessel (VV), VV Thermal Shield, Toroidal Field Coils and Central Solenoid Coils. Poloidal Field Coils, Cryostat and Cryostat Thermal Shield have not been involved . The structural design of those components can proceed only when Poloidal Field Coils sturcture has been determined according to requirements of the physical operation. The main components of CFETR show in Figure 3.

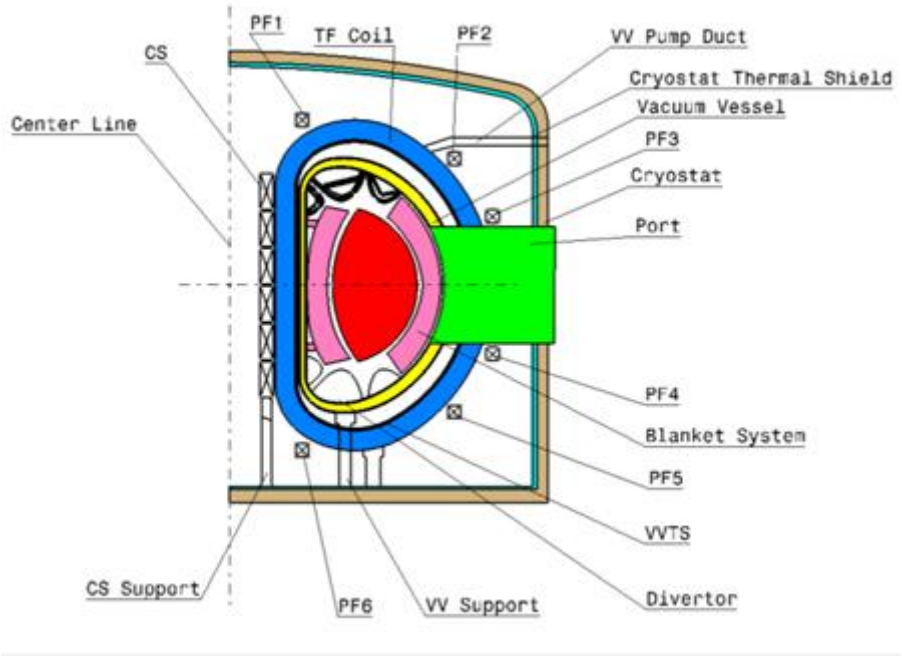

Figure 3 main components of the CFETR

Some important electromagnetic and mechanical characteristics of the magnet system arebased on the following parameters, which arelisted in Table 1.

Table 1 Preliminary schemes of the main components of CFETR

Large radius of plasma	$R = 5.5m$
Minor radius of plasma	$a = 1.6m$

Central magnetic field	*Bt = 4.5T/5.3T*
Elongation ratio	$\kappa = 1.8$
Triangle deformation	$\delta = 0.4$
Thickness of blanket	$about 0.8 \sim 1.0m$
Magnetic field ripple in the region of Plasma	<1%
Number of TF coils (N)	18

2.3.2 The basic structure TF coil for CFETR

To guarantee central field high enough, sufficient space for the cross-section of toroidalfield(TF) coil winding should be reserved, and a radial dimension of 750 mm is reserved. It is estimated that conductor designed for 60-70 kA could meet the total ampere turns current of coil winding, which is about 7800 kA to 9100 kA. (The total nominal current of ITER toroidal field coil winding is 9112 kA). The D-shaped cross-section of toroidal field magnet is composed of five arcs and one straight line which are tangent to each other. The length is about 700mm for one double-pancake winding. The space is 50mm between TF magnet and inner thermal shield for heat and electric insulation demand.

The inner side space of TF is 100mm for structure of central and hoop force. 100 mm of space inside the TF magnet is reserved for the centripetal-force-resisting support and toroidal support structure. The length of side plate is about 40mm and the length of inner plate is about 43mm to 73mm. A thickness of 40 mm is reserved for lateral plate of TF magnet, as well as about 43 to 73 mm for support plate inside. The dimension of winding cross section is about 536 mm × 618 mm. The D-shaped cross-section of TF magnet has yet to be optimized by Princeton-D pure tension coil theory. At present, the height and width is about 12m and 8m, respectively, for TF magnet.

The radial space of solenoid is scheduled for 490 mm. To guarantee the necessary magnetic flux, the inner diameter and outer diameter of central solenoid is scheduled for about 2300mm and 3280mm. The final dimension will be determined according to detailed analysis.

Figure 4is the general structure dimension of TF coil for CFETR.

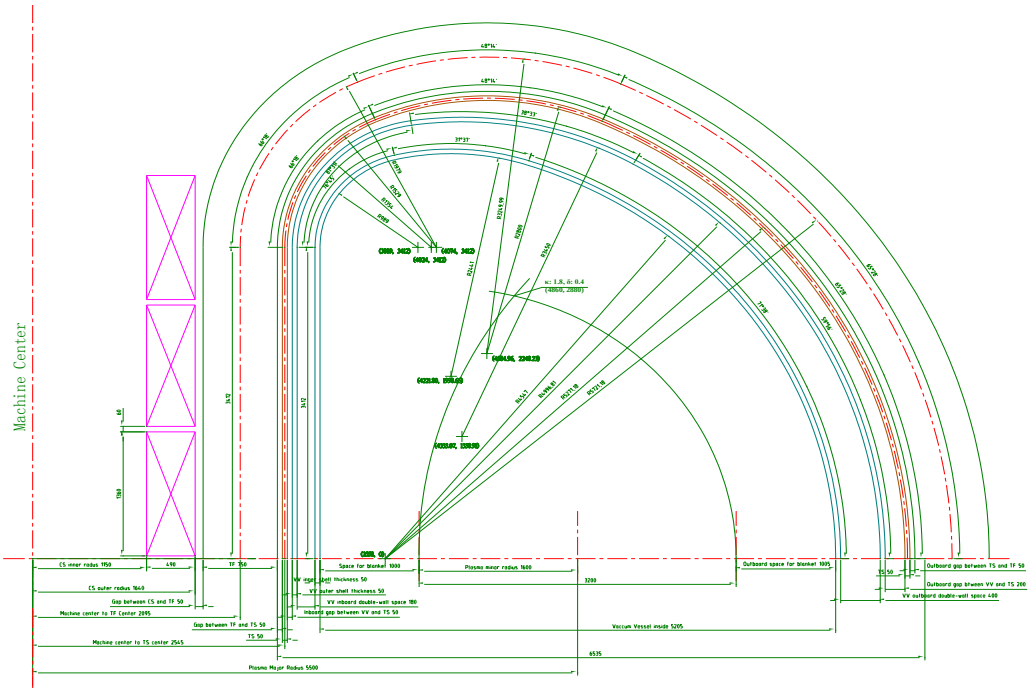

Figure 4 layout of the main components

2.3.3 The basic structure

Each TF coil consists of 130 turns. It is constituted by five same middle double layer coils (2 ×11 turns) and two double layer coils (2 +8 turns) located at the edge of each coil, as shown in Figure 4. The length of each of the five same middle double layer coils is about 660 m, while the length of each of the two marginal double layer coils is about 300m. Therefore, each coil has 6 layer joints and two terminal joints. The turn cross-section is about 536 mm ×618 mm. However, the specific size will be improved after finishing the design of conductor and insulation.

The basic design for both CFETR TF (for 1/18 model) and the section are shown in Figure 5 and Figure 6.

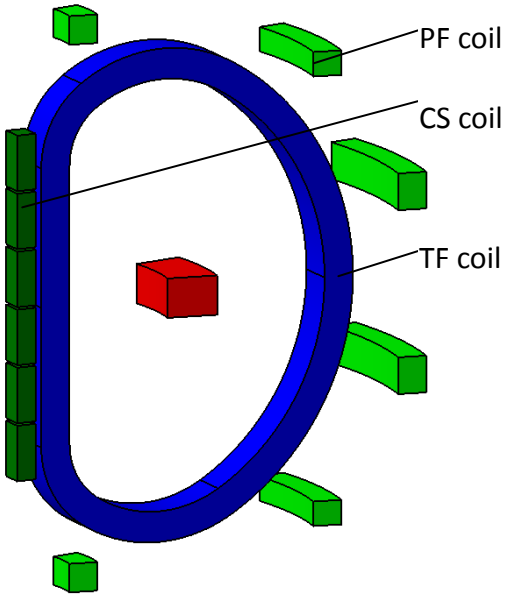

Figure 5 1/18 magnet system

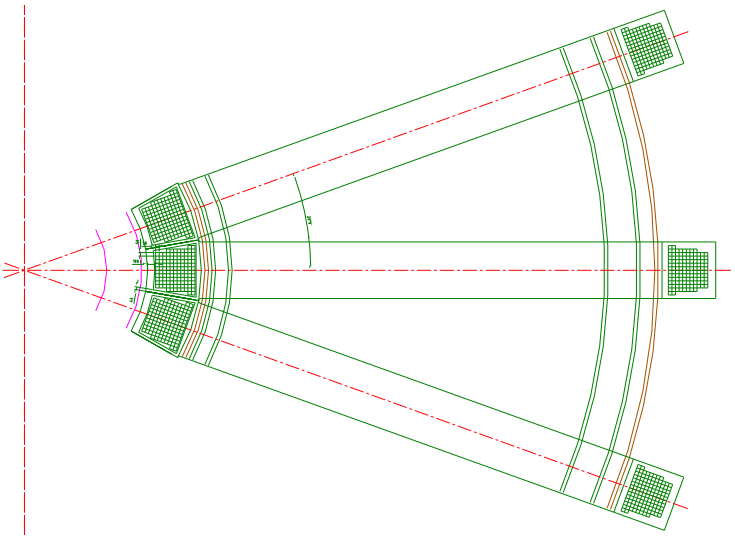

Figure 6 section of the TF coil

2.4 The analysis of the TF coil for the CFETR

2.4.1 The magnetic field distribution

This section summarizes the magnet calculation and analysis of the TF magnets in normal operation condition. Full detail of individual analysis (by magnetic codes) and analysis (mainly finite element analyses) is given in this section.

According to the relevant data mentioned above (such as the coil centerline and the cross-section parameters), a magnetic code was used to calculate the magnetic field distribution. The result is shown in Figure 7. It can be clearly found that the magnetic field of the plasma center is 4.5 T when the current of each turn reached to 53 kA. In addition, the maximum magnetic field was located at the inner side of the line segment of the coil, and the maximum magnetic field was about 10.5 T. Figure 7 also shows the distribution of magnetic field lines at equatorial plane on the right.

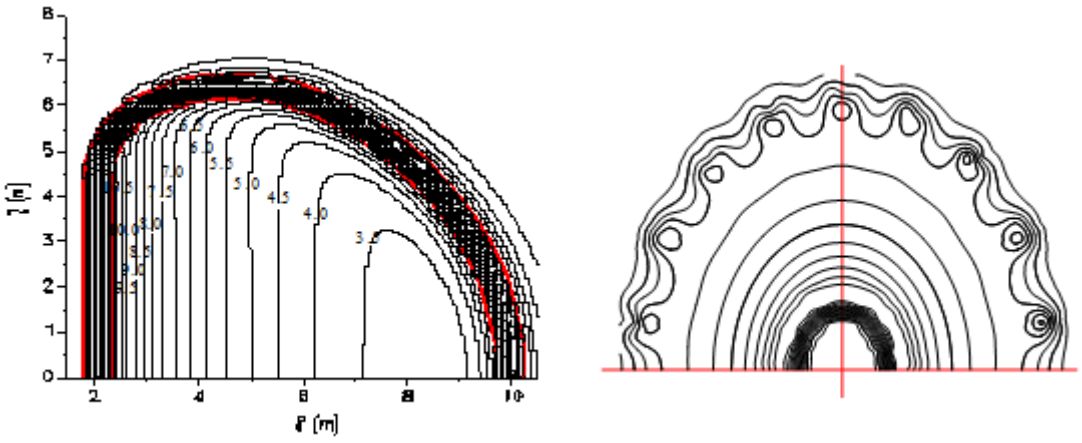

Figure 7 magnetic field distribution in vertical and equatorial plane

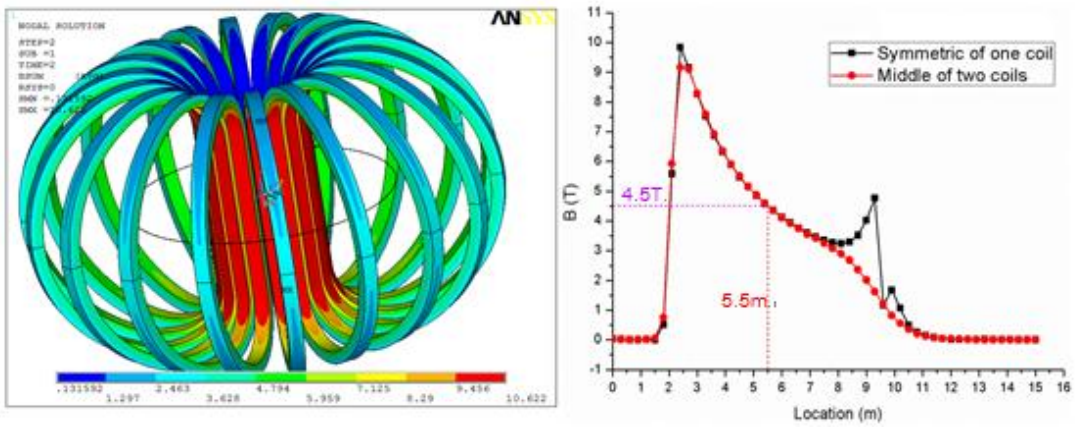

Figure 8 global magnetic field distribution and radial magnetic flux density curve

To validate the reliability of the results which was calculated by the magnetic codes, ANSYS was used to perform further analysis. Figure 8 gives the distribution of the magnetic field. Besides, the magnetic field's curve with the radius on the equatorial plane can be shown on the right. The maximum magnetic flux density is about 10.6 T and the magnetic field of the plasma center is 4.5 T when the current of each turn is 53kA. Both of the results are similar to the results calculated by magnetic code.

2.4.2 The magnetic field ripple in the region of Plasma

As TF coils is discrete distribution along the circumference, the magnetic field at the same radius is not the same in different directions along circumference, and thus there is ripple. Ripple is defined as follows:

$$\delta(r,z)=\frac{B_{\varphi}^{\max}-B_{\varphi}^{\min}}{B_{\varphi}^{\max}+B_{\varphi}^{\min}}$$

Where $B_{\varphi}^{\max}$ and $B_{\varphi}^{\min}$ are the maximum and minimum magnetic field of the (r,z) position. For the coordinate system, $B_{\varphi}^{\max}$ and $B_{\varphi}^{\min}$ will appear in the plane $\varphi=0^{\circ}$ and $\varphi=10^{\circ}$. Figure 4.5 shows the TF magnetic field ripple which is calculated by a computer

program. The result shown in Figure 9 indicates that ripple near 0% in the circle area where the center of the circle area is estimated to be (5.5, 0) with a radius of 1.6 m. And the ripple in marginal region of the plasma is near 1% due to the aspect ratio (R / a =5.5 m /1.6 m).

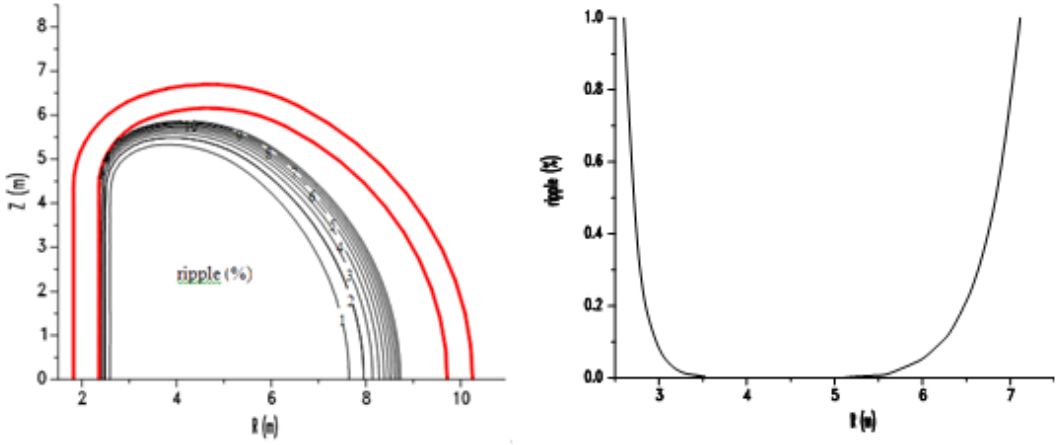

Figure 9 ripple distribution in the vertical plane and along the radial direction

2.4.3 analysis of electromagnetic force

Each TF coil experiences a bursting force as well as a resultant centering force towards the center of the machine. The resultant centering forces are reacted by the cylindrical vault formed by the inboard straight legs of the TF coils. The bursting force on each coil is reacted by a combination of the coil case and winding pack. The magnetic forces occur on the winding pack, and the winding pack tends to be pushed outwards against the outer case ring. The overall coil centerline shape is more vertically elongated than that of the idealized “bending moment force” shape for an 18 coils TF system and it is actually chosen to satisfy the plasma ripple requirement and the vertical divertor space. TF coil will generate expansion force since its own magnetic field. In addition, the synthesis of the electromagnetic force will point to the inside of the coil due to the fact that the inside magnetic field stronger than the lateral magnetic field of the coil. Thus, centripetal force will be formed. Figure 10 shows the electromagnetic force of the TF

coil. The centripetal force is about 290MN when the current of each turn is 53kA, while the tensile force formed by a half coil, which is perpendicular to the equatorial plane, is about 128MN. However, the overturning torque of the coils can be calculated only after designing the PF coil's current.

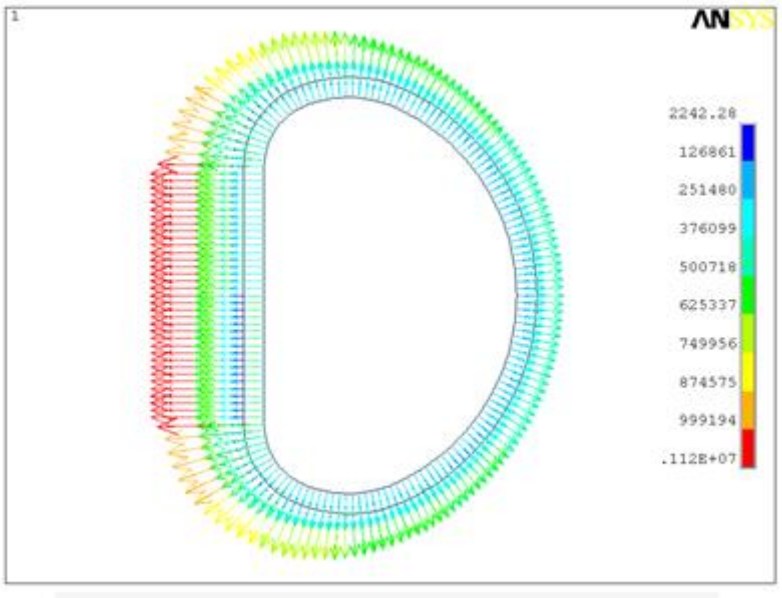

Figure 10 EM force on the TF coil

Inductance and energy storage of TF coil is shown in Table 2, when coil current 62.25kA, its stored energy was calculated as follows:

$$W = \frac{1}{2} LI^2 \quad =31.2\text{GJ}$$

Table 2 inductance of the #1 TF coil and other 17 TF coils

Coil	1	2&18	3&17	4&16	5&15	6&14
Inductance (H)	0.317	0.117	0.0606	0.0354	0.0223	0.015
Coil	7&13	8&12	9&11	10	Total	
Inductance (H)	0.0107	0.00833	0.00708	0.00670	15.78	

2.4.4 Results of 5.3T design parameter

With the 5.3T design parameter, using the same method based on ANSYS, another electromagnetic analysis has been performed. When the current of each turn is 62.25 kA, the maximum magnetic flux density is about 12.5 T and the magnetic field of the plasma center is 5.3 T. Considering the critical magnetic field value of the superconductor material is lower than 12T, this 5.3T design parameter is not suitable for engineering requirement. Figure 4.8 gives the distribution of the magnetic field. Besides, the magnetic field's curve with the radius on the equatorial plane can be shown in Figure 11.

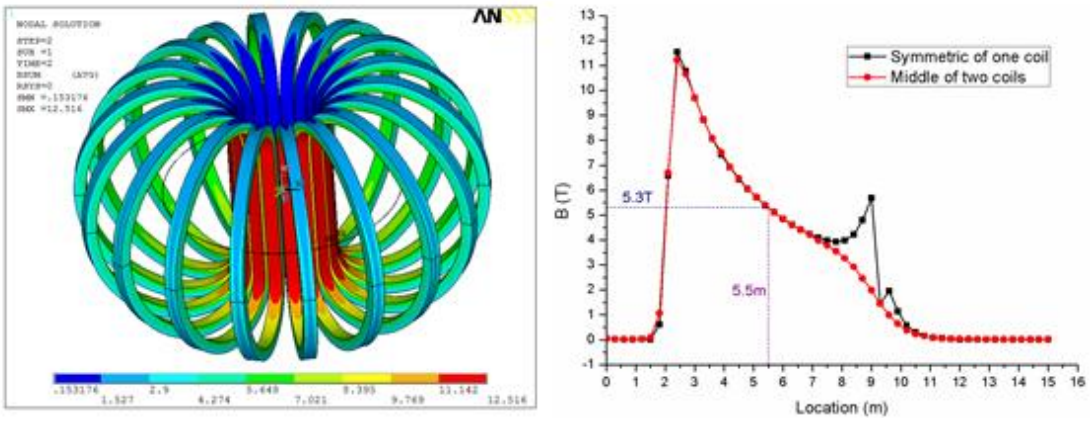

Figure 11 magnetic field distribution and radial magnetic flux density curve in the 5.3T case

Table 3 gives the geometry parameters and analysis results of CFETR TF coil, and it was compared with the parameters of the ITER TF coil.

Table 3 TF coil parameters

	CFETR	ITER
Coil number	18	18

turns	130		134
R	5.5m		6.2m
Current	53kA	62.25kA	68kA
Center magnet	4.5T	5.3T	5.3T
Maximum magnet	10.6T	12.5T	11.8T
inductance	15.78H	15.78H	17.7H
energy storage	22.2 GJ	30.6GJ	41GJ
centripetal force	290 MN	367MN	403MN
Vertical force	128 MN	175MN	205MN

2.4.5 Conclusion

The current of the TF coil is 53kA; the maximum magnetic flux density of the TF magnet coil is 10.6T; and the magnetic flux density of its center is 4.5T. the centripetal force is about 290 MN when the current of each turn is 53 kA, while the tensile force formed by a half coil, which is perpendicular to the equatorial plane, is about 128 MN. It is concluded that when the TF coil current is 53kA, this will meet the requirements.

2.5 Candidate schemes of the TF coil for the CFETR

Toroidal field generated by the TF coil can be estimated through the application of Ampere's law (The smaller the magnetic field ripple of the area is, the more accurate the estimation will be). Ampere's law is expressed this way: in a static magnetic field, the line integral of magnetic field strength (H stand for it) along any closed path is equal to the total current surrounded by the closed path. Its mathematical equation is as follows: $\oint \vec{H} \cdot d\vec{l} = \sum i$, that is $\oint \vec{B} \cdot d\vec{l} = \mu_0 \sum i$

where $\mu_0 = 4\pi \times 10^{-7}$ is the vacuum permeability.

It is approximately assumed that 18 TF coils form an axially symmetric system, and the above equation can be written as:

$2\pi RB = \mu_0 I$, that is $B = \frac{\mu_0 I}{2\pi R}$

Where I is the total number of ampere turns of the 18 coils.

Figure 12 shows four kinds of constant tension D-shaped curve of CFETR TF coil. The design principles are based on the D-shaped curve designed by Wu Songtao. Considering the size, location and assembly of other main components of CFETR such as vacuum vessel, diagnose ports, blanket and so on, the four kinds of constant tension D-shaped curve are designed as follows: the inside straight line segment of the D-shaped curve is fixed, while the outer arc segment is stretched outwards.

To obtain magnetic field distribution, analysis has been performed for the four kinds of TF coil. All of the three TF coil were analyzed at the condition of 53 kA/turn. Results show that the maximum magnetic flux density and the magnetic flux density of the center of plasma of the four kinds of TF coil are almost similar with results of the D-shaped curve designed by Wu Songtao.

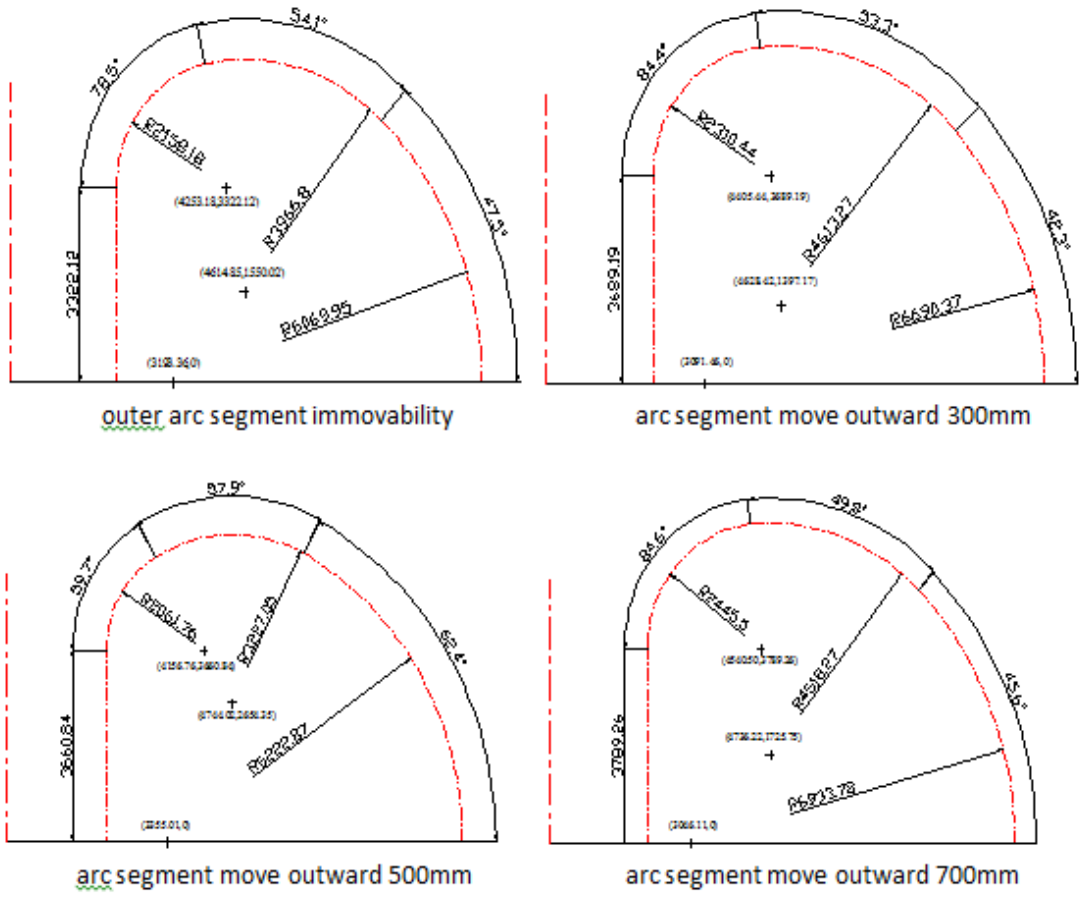

Figure 12 candidate profiles of the TF coil

2.6 Summary

This report gives a brief view of the conceptual design for CFETR TF. The current of the TF coil is 53kA; the maximum magnetic flux density of the TF magnet coil is10.6T; it is concluded that when the TF coil current is 53kA, this will meet the requirements. However, candidate schemes of the TF coil for the CFETR have been designed to consider the size, location and assembly of other main components of CFETR such as vacuum vessel, diagnose ports, blanket and so on. The analysis works help to confirm and optimize the design structure.

3 PF&CS coils

3.1 Purpose

Plasma equilibrium calculation was done to made sure the PF and CS coils location and current, EM analysis was done to support help for optimizing the location and the section size for the PF and CS coils.

3.2 Introduction

A series of plasma equilibrium calculation were carried out for China Fusion Experimental Tokamak Reactor (CFETR), based on the designed main parameters and optimized poloidal field (PF) coils parameters. These plasma equilibria calculations for machine design have been developed with EFIT boundary fitting mode (R-file). The machines specific parameters for CFETR must be modified to build a correct modeling. All converged plasma equilibrium solutions are free boundary equilibria in that the coil currents and resulting plasma obey the Grad-Shafranov equation. In boundary fitting mode, a series of points on a target plasma boundary are used to constrain the plasma equilibrium shape to match this target geometry. Then, the PF coil currents and unknown plasma parameters can be determined to best match the target shape in a least square sense. As for machine design, the target shape is always the desired design shape for future experiment.

After plasma equilibrium calculation, electromagnetic analysis for PF coils and CS modules are determined the maximum magnetic flux density, which can guide to optimize the location and the section size for the PF coils and CS coils.

3.3 Main parameters

The main parameters of the concept design for CFETR are summarized in Table 4.

Table 4 CFETR main parameters

Plasma current Ip	10 ~ 12 MA
Major radius R	5.5 m
Minor radius a	1.6 m
Toroidal field Bt	4.5/5.3T @5.5m
Elongation κ	1.8
Triangularity δ	0.4

3.4 Desired plasma shape and designed PF and CS coils

Based on physics design, two magnetics-constrained, fully converged, free boundary equilibria were produced: a Lower Single Null (SN) and a Double Null (DN) configuration. PF and CS coils parameters are summarized in Table 5. Desired plasma shape and designed PF and CS coils in CEFTR geometry are shown in Figure 13.

Table 5 initial PF&CS coil geometry parameters

Coil	R[m]	Z [m]	dR [m]	dZ[m]
CS3U	1.395	3.55	0.49	1.36
CS2U	1.395	2.13	0.49	1.36
CS1U	1.395	0.71	0.49	1.36
CS1L	1.395	-0.71	0.49	1.36
CS2L	1.395	-2.13	0.49	1.36
CS3L	1.395	-3.55	0.49	1.36

PF1	3.35	6.46	1.5	1.1
PF2	8.35	5.25	0.5	0.5
PF3	9.93	2.75	0.5	0.5
PF4	9.93	-2.75	0.5	0.5
PF5	8.35	-5.25	0.5	0.5
PF6	3.35	-6.46	1.5	1.1

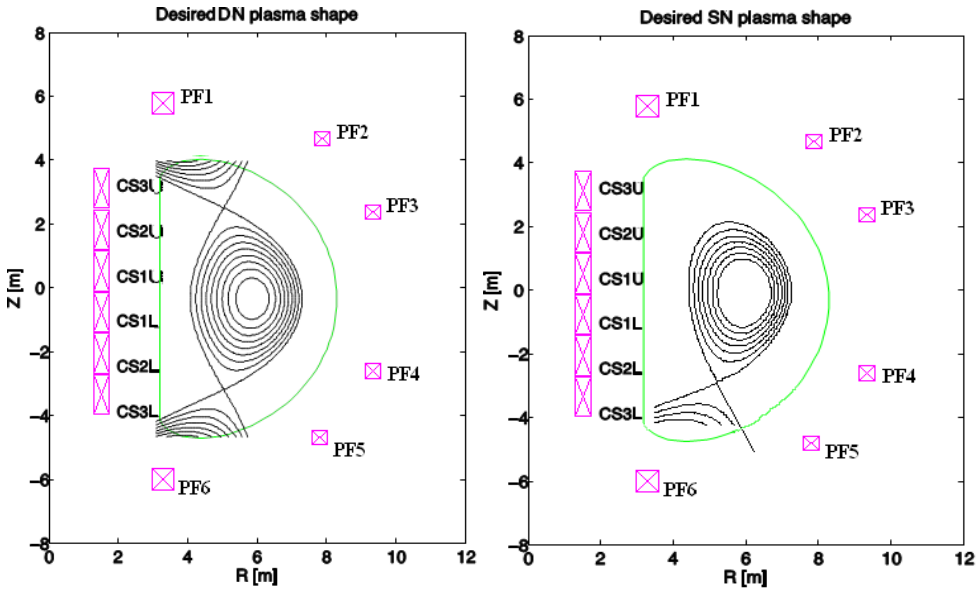

Figure 13 different plasma shape and PF&CS layout (left: double null shape, right: single null shape)

3.5 4. Plasma equilibria calculation and EM analysis for PF and CS coils

3.5.1 Plasma equilibria results

Based on the designed main parameters and target plasma shape, a series of plasma equilibria solutions are summarized here. Table 6 shows the plasma equilibrium parameters for 10MA plasma discharge, and the corresponding PF coil currents are

shown in Table 7. The plasma equilibrium parameters and PF coil currents for 12MA plasma discharge are summarized in Table 8 and Table 9.

As shown in Table 3 and Table 5, the plasma equilibrium parameters are almost same with each other, because of the same desired plasma shape constrain (Fig. 1). Only small geometry difference exists. For example, the X point locations have $1 \sim 5cm$ difference between the desired value ($\left(4.86m, \pm 2.88m\right)$) and the equilibrium solutions. In Table 6 and Table 8, only low X-point is shown for DN configuration, where the upper one has a symmetric value about the middle plane.

The PF and CS coils currents are shown in Table 7 and Table 9, which are the shaping currents with almost zero volt seconds contribution to these plasma equilibrium solutions.

Table 6 10MA plasma equilibrium parameters

	Design	**R[m]**	**a[m]**	β_P	l_i	δ_u/δ_l	k	**Rxp [m]**	**Zxpt[m]**
DN	1	5.5	1.6	0.9	1.0	0.4	1.80	4.86	-2.89
SN	1	5.5	1.59	0.87	1.0	0.2/0.4	1.75	4.84	-2.91

Table 7 PF&CS coil current in 10MA plasma scenario (MA*turns)

	Design	**CS3U/3L**	**CS2U/L**	**CS1U/L**	**PF1/PF6**	**PF2/PF5**	**PF3/PF4**
DN	1	-18.63	-21.53	-4.07	24.68	-6.64	-2.80
SN	1	-5.43/ -8.76	-10.10/ -16.78	-9.06/ -12.35	5.76/ 17.52	-1.45/ -2.89	-4.14/ -4.81

Table 8 12MA plasma equilibrium parameters

	Design	**R[m]**	**a[m]**	β_P	l_i	δ_u/δ_l	k	**Rxp [m]**	**Zxpt[m]**
DN	1	5.5	1.6	0.9	0.96	0.4	1.8	4.86	-2.89
SN	1	5.5	1.6	0.86	0.93	0.2/0.4	1.70	4.85	-2.90

Table 9 PF&CS coil currents in 12MA plasma scenario (MA*turns)

	Design	CS3U/3L	CS2U/L	CS1U/L	PF1/PF6	PF2/PF5	PF3/PF4
DN	**1**	**-21.48**	**-32.47**	**-1.24**	**31.82**	**-8.98**	**-2.89**
SN	1	-9.37/ -13.36	-14.96/ -25.67	-6.46/ -11.65	8.94/ 25.07	-2.78/ -5.69	-4.52/ -4.57

3.5.2 EM result onto the PF and CS coils

Basing on the Plasma equilibria calculation, it has made sure the preliminary PF and CS coils current, it also should obtain the magnetic field. The aims for electromagnetic analysis for PF coils and CS modules are determined the maximum magnetic flux density, which can guide to optimize the location and the section size for the PF coils and CS coils.

It takes the data of Table 912MA DN as the electromagnetic analysis, because it has the maximum current load.

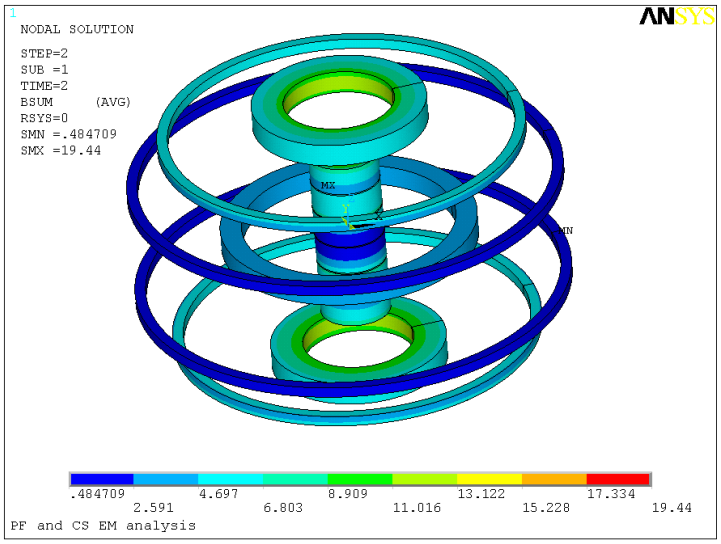

Figure 14magnetic flux density distribution on the PF&CS coils

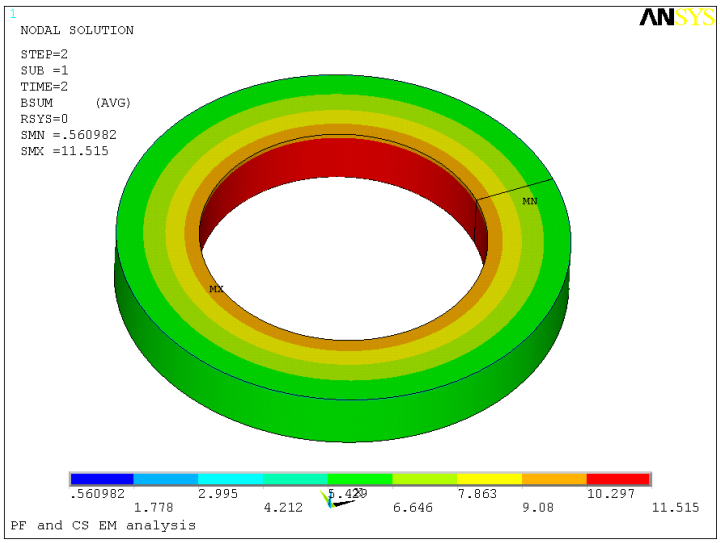

Figure 15 magnetic flux density distribution on the PF1 coil

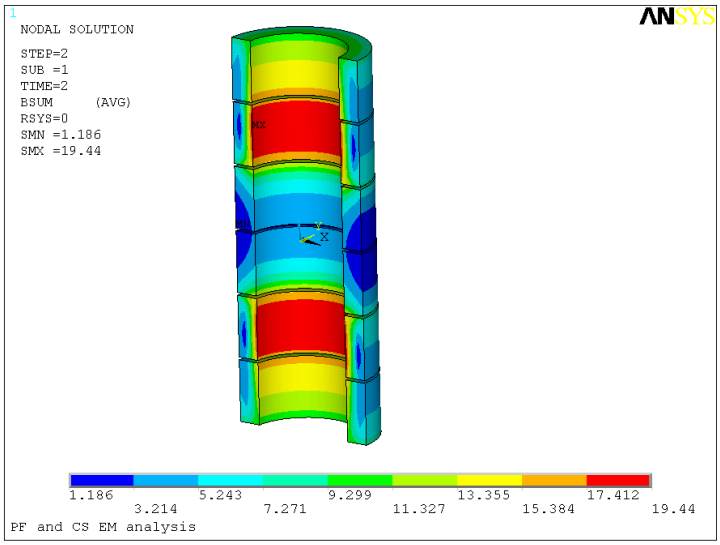

Figure 16 magnetic flux density distribution on the 6 CS coils

As shown in Figure 14 and Figure 15, the maximum total magnetic field is 11.5T on the inner curved parts for the PF1 and PF6. Because it is hoped to use NbTi cable-in-conduit conductors for the PF, it is thought the magnetic flux density is to higher, the magnetic flux density for PF1 and PF6 should be decreased. The maximum

total magnetic field is 19.4T on the inner curved parts for the CS2U and CS2L, it also is thought the magnetic flux density is to higher.

Conclusion, basing on theplasma equilibrium calculation, it has obtained PF and CS current, but the EM analysis results show that the maximum magnetic field for PF and CS are too higher, which should be decreased.

3.5.3 Plasma equilibria results with adjusted the PF1/6 coils location

As described in previous section, a series of plasma equilibrium solutions based on the designed plasma shape and different PF coils design are shown. In order to satisfy the desired plasma shape, some PF coils should afford high current, especially in DN configuration of 12MA plasma discharge, such as CS2U/D, PF1 and PF6.

In order to reduce the power requirements, some PF coils parameter should be adjusted. For example, reduce the Z coordinate of PF1 and PF6 by 46cm based on Design 1, as shown in Figure 17. A plasma equilibrium solution of 12MA plasma discharge with DN configuration is calculated and summarized in Table 10 and Table 11. The equilibrium solution gives the same plasma shape, but the required current on PF1 and PF6 reduces a lot, from 31.82 MA*turns (4th line in Table 8) to 25.86 MA*turns (Table 10). But, other coils, such as CS3U/L and CS2U/L still required high current. So, more coils parameters should be adjusted.

Table 10 12MA DN plasma equilibrium parameters

	Ip [MA]	**R[m]**	**a[m]**	β_P	l_i	δ_u/δ_l	k	**Rxp [m]**	**Zxpt[m]**
DN	12	5.5	1.6	0.9	0.96	0.4	1.8	4.86	-2.89

Table 11 PF&CS coil currents in 12MA DN plasma scenario (MA*turns)

CS3U/CS3L	CS2U/CS2L	CS1U/CS1L	PF1/PF6	PF2/PF5	PF3/PF4
-23.89	-32.29	-1.05	25.86	-7.73	-3.20

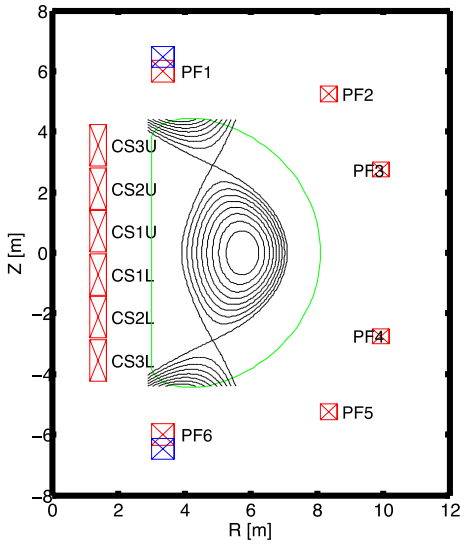

Figure 17 DN plasma shape with lower PF1 and PF6 coils (blue: previous position, red: current position)

3.5.4 Plasma equilibria results with adjusted the PF and CS coils location

3.5.3shows a possible way to reduce the coils current requirements. Another two PF coils upgrade scheme based on Design 3 were carried out, the corresponding PF coil parameters are shown in Table 12. A comparison of PF coils Design 1 (Red) and these two upgrades (Named as Design1_Mod1 (Blue)) are shown in Figure 18.

Table 12 adjusted PF&CS coil positions

Coil	R[m]	Z [m]	dR [m]	dZ[m]
CS3U	1.339	3.85	0.49	1.50

CS2U	1.339	2.31	0.49	1.50
CS1U	1.339	0.77	0.49	1.50
CS1L	1.339	-0.77	0.49	1.50
CS2L	1.339	-2.31	0.49	1.50
CS3L	1.339	-3.85	0.49	1.50
PF1	3.00	6.16	1.5	1.1
PF2	8.02	4.85	0.5	0.5
PF3	9.865	1.75	0.5	0.5
PF4	9.865	-1.75	0.5	0.5
PF5	8.02	-4.85	0.5	0.5
PF6	3.00	-6.16	1.5	1.1

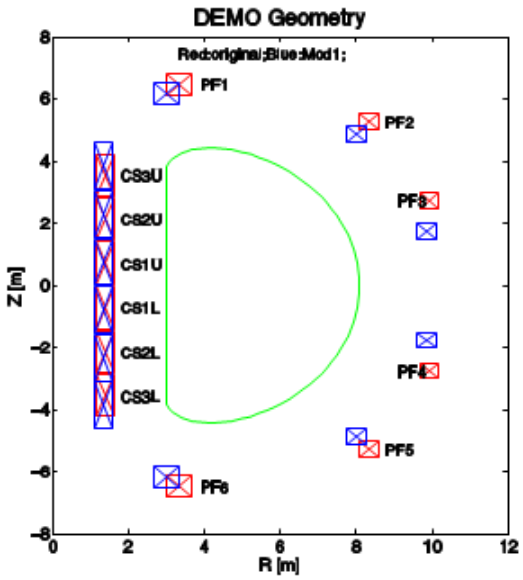

Figure 18 comparison of the PF&CS coil position (red: previous position, blue: current position)

As shown in Figure 18, these two upgrades make the PF1~PF6 coils more close to plasma, and take the CS coils slightly away from plasma (6cm reduction in R direction) but area added.

3.5.5 Plasma equilibrium solutions based on desired plasma shape

Here, the plasma equilibrium solutions for 12MA plasma discharge with DN configuration based on desired plasma shape shown in Figure 13 are summarized in Table 13 and Table 14. The current on coils are not changed much for this desired plasma shape, and some coil currents are required even more, such as CS2U/L.

Table 13 12MA plasma equilibrium parameters

	Design	**R[m]**	**a[m]**	β_P	l_i	δ_u/δ_l	k	**Rxp [m]**	**Zxpt[m]**
DN	Design1	5.5	1.6	0.9	0.96	0.4	1.8	4.86	-2.89
	Mod1	5.5	1.6	0.9	0.96	0.4	1.8	4.86	-2.89

Table 14 PF&CS currents in 12MA DN plasma scenario (MA*turns)

	CS3U/CS3L	**CS2U/CS2L**	**CS1U/CS1L**	**PF1/PF6**	**PF2/PF5**	**PF3/PF4**
Design1	-21.48	-32.47	-1.24	31.82	-8.98	-2.89
Mod1	-23.75	-41.38	-1.68	34.34	-7.50	-2.65

It find that the current change a little if it only adjusts the location of PF and CS coils, the maximum magnetic field will be very high, it shows that it has little function to reduce the magnetic field if only adjusts the location of PF and CS coils.

3.5.6 Plasma equilibrium result with new DN desired shape

In order to reduce the PF coils current requirements, a new desired plasma shape in

DN configuration was developed as shown in Figure 19. The main modifications are elongation (from 1.8 to 1.95), X-points location (from (4.86m, 2.88m) to (4.70m, 3.00m)), and the triangularity (from 0.4 to 0.5). The equilibrium parameters are summarized in Table 15, and the corresponding PF coil currents are shown in Table 16.

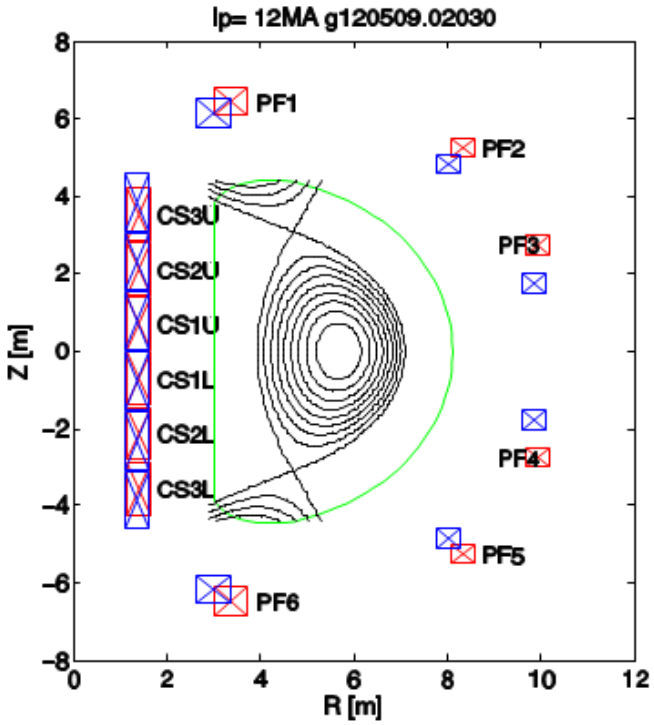

Figure 19 proposed DN plasma shape

Table 15 plasma equilibrium parameters with the proposed plasma shape

		R[m]	a[m]	β_P	l_i	δ_u/δ_l	k	Rxp [m]	Zxpt[m]
10MA	Design1	5.51	1.59	0.9	1.1	0.46	1.93	4.77	-3.08
	Mod1	5.51	1.59	0.9	1.1	0.51	1.95	4.70	-3.09
12MA	Design1	5.52	1.58	0.9	0.97	0.50	1.95	4.77	-3.08
	Mod1	5.52	1.58	0.9	0.98	0.52	1.96	4.70	-3.09

Table 16 PF&CS coil currents in the proposed plasma shape

		CS3U/L	CS2U/L	CS1U/L	PF1/PF6	PF2/PF5	PF3/PF4
10MA	Design1	-12.21	-11.96	-11.04	15.86	-3.52	-3.95
	Mod1	-11.27	-13.42	-13.95	15.95	-3.67	-2.98
12MA	Design1	-15.74	-15.36	-12.49	20.20	-5.02	-4.29
	Mod1	-14.49	-17.18	-16.06	20.13	-4.88	-3.32

After changing the desired plasma shape, the coil current on PF coils reduce much, especially in CS3U/L, CS2U/L and PF1, PF6.

3.5.7 EM result onto the updated PF/ CS coils and updated plasma shape

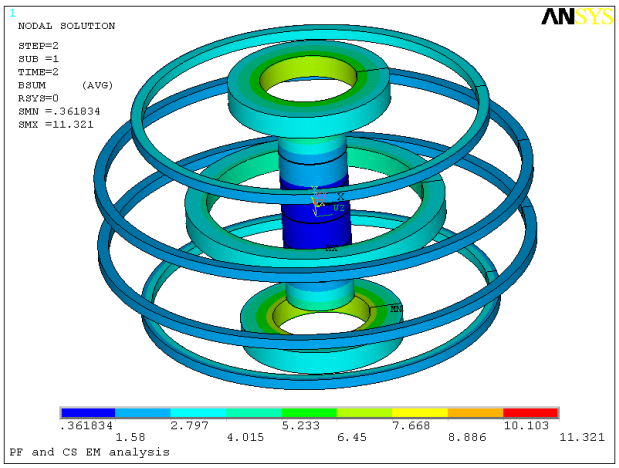

Figure 20 magnetic flux density distribution on the PF&CS coils

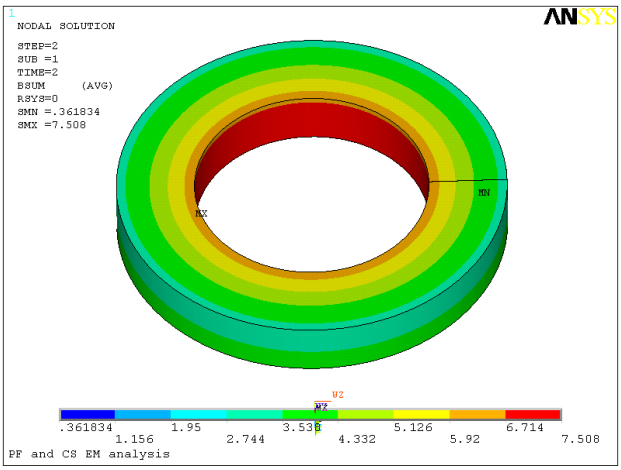

Figure 21 magnetic flux density distribution on the PF1 coil

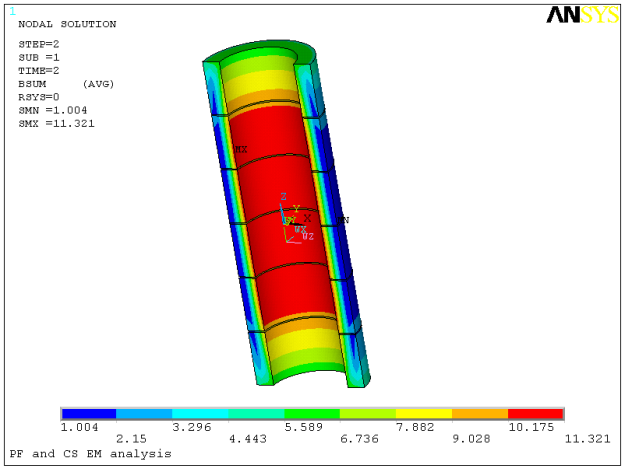

Figure 22 magnetic flux density distribution on the 6 CS coils

As shown in Figure 21 and Figure 22, the maximum total magnetic field is 7.5T on the inner curved parts for the PF1 and PF6. It is thought the magnetic flux density is a little higher, this value would be more reasonable if it is smaller than the 7T. The maximum total magnetic field is 11.3T on the inner curved parts for the CS2U, it is thought the magnetic flux density is reasonable.

Table 17 PF&CS coil EM force

Coil	MAG

	Fz(MN)
PF1	-139.5
PF2	39.7
PF3	-6.48
CS3U	308
CS2U	86.1
CS1U	-1.9

Table 18updated PF1 and PF6 dimensions

Coil	R[m]	Z [m]	R [m]	Z[m]
PF1	3.0	6.16	1.7	1.2
PF6	3.0	-6.16	1.7	1.2

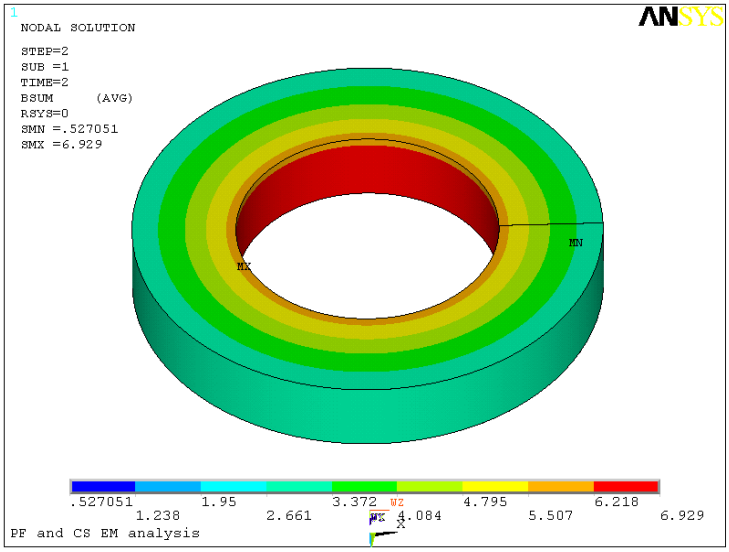

Figure 23 magnetic flux density distribution on the PF1 coil

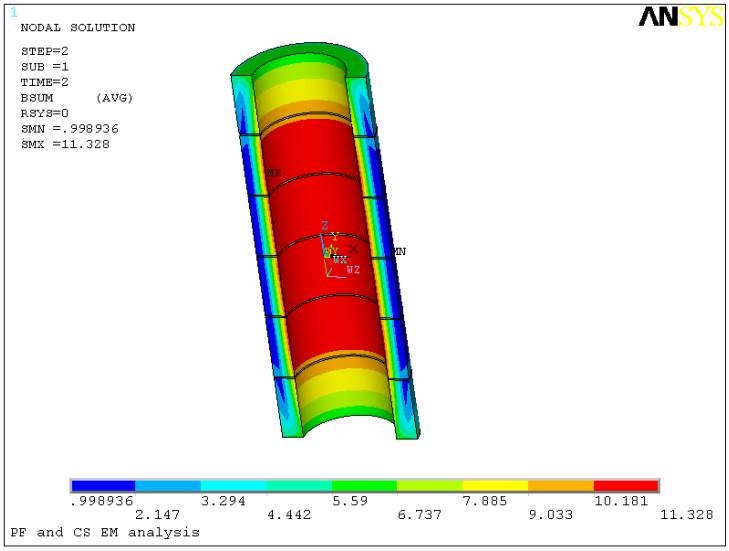

Figure 24 magnetic flux density distribution on the 6 CS coils

As shown in Figure 23 and Figure 24, the maximum total magnetic field is 6.93T on the inner curved parts for the PF1 and PF6. It is thought the magnetic flux density is reasonable. The maximum total magnetic field is 11.3T on the inner curved parts for the CS2U, it is thought the magnetic flux density is reasonable.

Conclusion, adjusted plasma shape would reduce the PF and CS coils current deeply, but it is still high for the magnetic field of PF1/6 and increasing the section dimension for PF1/6 would reduce the magnetic field of PF1/6.

3.6 Preliminary calculated for Volt seconds of PF and CS coils

Volt seconds is about 100Vs, it is not beyond 15GS for the stray magnetic field at the plasma region (R5500mm,a1600mm)

Table 19 PF&CS coil geometry and current

Coil	R[m]	Z [m]	dR [m]	dZ[m]	Current(MAt)
CS3U	1.339	3.85	0.49	1.50	13.20

CS2U	1.339	2.31	0.49	1.50	10.87
CS1U	1.339	0.77	0.49	1.50	10.86
CS1L	1.339	-0.77	0.49	1.50	10.86
CS2L	1.339	-2.31	0.49	1.50	10.87
CS3L	1.339	-3.85	0.49	1.50	13.20
PF1	3.00	6.16	1.5	1.1	6.24
PF2	8.02	4.85	0.5	0.5	0.37
PF3	9.865	1.75	0.5	0.5	0.15
PF4	9.865	-1.75	0.5	0.5	0.15
PF5	8.02	-4.85	0.5	0.5	0.37
PF6	3.00	-6.16	1.5	1.1	6.24

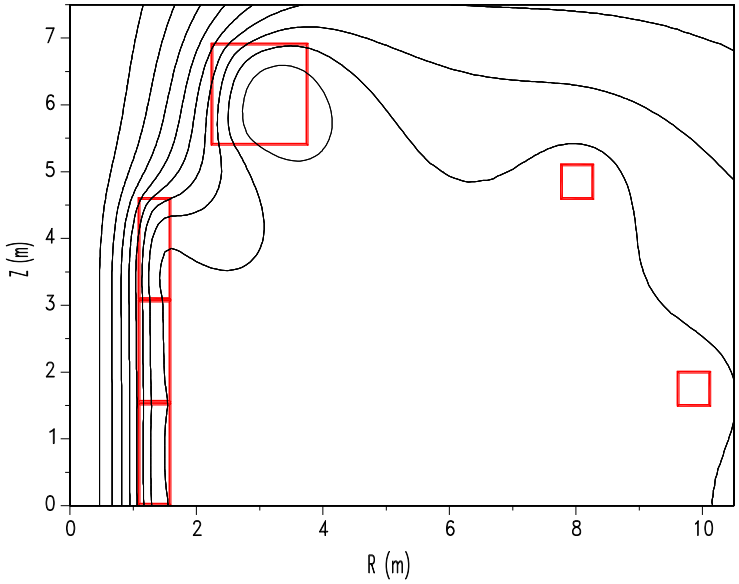

Figure 25 magnetic contour line

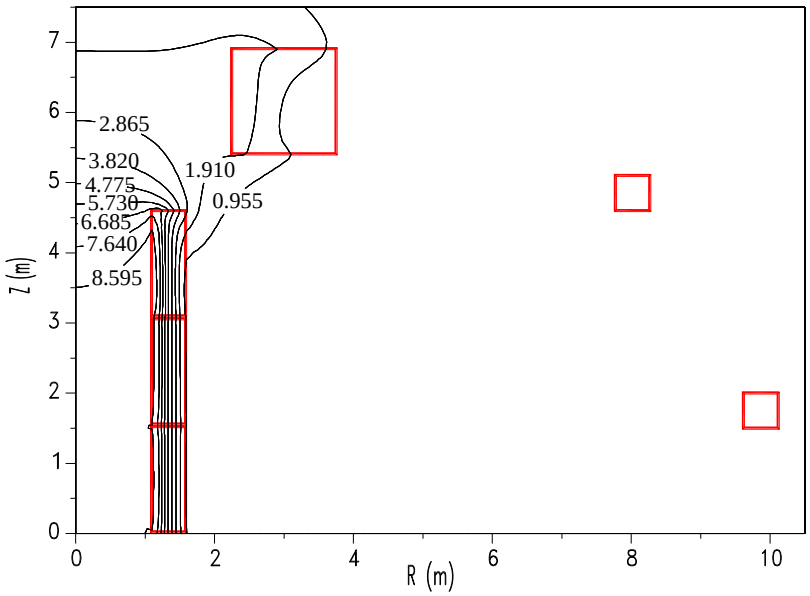

Figure 26 magnetic flux density distribution

As shown in Figure 25, the maximum total magnetic field is 2.5T on PF1. The maximum total magnetic field is 9.55T on the CS coils.

Table 20 magnetic field and flux at specified postions

Point location	magnetic field (GS)	magnetic flux(Wb)
(3.9,0)	1.491	50.013
(5.5,0)	2.853	50.039
(7.1,0)	0.304	50.053
(4.5,1.3)	7.987	50.017
(5.5,1.6)	5.471	50.039
(6.0,1.5)	4.123	50.027

3.7 Summary

A series of plasma equilibrium solutions for CFETR 10MA and 12MA plasma discharge were shown. Based on three PF coil designs, the coil currents correspond to

the 10MA and 12MA plasma equilibrium in DN and SN configuration are given, which provide a good evaluation for these PF coils design. In order to reduce the coil current requirements, a new desired plasma shape in DN configuration is developed, which makes the original designed plasma parameters in its geometry changes a lot.

After make sure the PF and CS coils current, magnetic field analysis was done, the result show that the dimension in table 9 is more reasonable, but for PF1/PF6 should be replaced by Table 15. The preliminary Volt seconds is about 100Vs and satisfies the requirement.

Certainly，it still should be a further optimization about the desired plasma parameters, the PF and CS coils.

4 Vacuum vessel

4.1 Introduction Functions and Design Requirements

This report is to describe the conceptual design for Vacuum Vessel of CFETR (China Fusion Engineering Test Reactor). It gives a comparison between the ITER VV and CFETR VV to show the different and optimization for the CFETR VV. The conceptual design includes the VV D-shape, the shell structure, the port layout, the rib layout, the blanket support change and the cooling flow system. The basic goal for the VV is to ensure that the temperature of the inner shell is 500℃and the outer shell is at 100℃. To achieve this goal, the conceptual design is optimized and the analysis simulation would confirm the design.

The Vacuum Vessel is a part of the CFETR and consists of the following sub components: **the main vessel, port structures, support structuresfor in-vessel components, and the VV coolant system interface.**

4.1.1 Functions

1. Provide the first confinement barrier for radioactive materials.
2. Remove decay heat of all in-vessel components, even in conditions when the other cooling systems are not functioning.
3. Provide a boundary consistent with the generation and maintenance of a high quality vacuum.
4. Mount in-vessel components and support electromagnetic loads during plasma disruptions and vertical displacement events.
5. Together with the first wall and blanket, maintain a specified toroidal electrical resistance and contribute to plasma stability.

6. Together with the first wall, blanket, divertor, and ancillary equipment in ports, provide adequate radiation shielding for the superconducting coils.

7. Provide access ports for in-vessel components maintenance equipment, diagnostics and plasma heating methods, and blanket test modules.

4.1.2 Design Requirements

General Requirements

1. Provide the first strong barrier for the reactor and withstand accidents without losing confinement. This is to reduce the potential for the release of radioactive materials and ensure that any releases are within prescribed limits.

2. Provide a reliable structural boundary for the lifetime of the reactor.

Vacuum Requirements

1. The VV shall provide a continuous welded wall for tritium containment.

2. The design and construction of the Vacuum Vessel shall be consistent with providing a high quality vacuum.

3. The vacuum duct size and number, material choice and design of the in-vessel components, and the gap size between all in-vessel components shall be compatible with ultra high vacuum requirements

Structural Requirements

The vacuum vessel must withstand the following loads:

1. All possible combinations of internal and external pressure due to off-normal conditions such as coolant (water) or cryogenic fluid leakage

2. Electromagnetic loads.

3. Weight of internal components and self-weight

4. Forces induced on the internal components, blanket back plate and divertormounts, that are transmitted to the VV.

5. Forces applied during installation and removal of in-vessel components.

6. Seismic loads on the vessel and seismic loads transmitted to the VV from the

in-vessel components.

7. Must withstand thermal loads consistent with the requirements

8. Coolant pressure

Electromagnetic Requirements

The VV shall support electromagnetic loads during plasma disruptions, vertical displacement events (VDE), and fast discharge of the TF Coils.

Thermohydraulic Requirements

1. The VV must be cooled to remove normal and off normal heat from the system.

2. The inner surface of the VV should be kept above 770K to reduce the tritium deposition, while the outer surface of the VV, which faces the VVTS should be kept below 373K to minimize the radiation heat load to the thermal shield.

3. Bulk boiling is not allowed during normal operation or baking.

4. For decay heat removal, the cooling system shall make use of natural convection, and the maximum cooling capability shall be 3 MW.

5. The heat shall be removed by two independent cooling systems, to minimize the effect of faults.

6. The vacuum vessel shall be connected to a suppression tank (pool) with rupture disks in order to limit the internal pressure in case of loss of coolant from in-vessel components to 0.5 MPa.

Mechanical Requirements

1. Enough space shall be provided between the VV and 4 K components to allow space for the thermal shield with clearances in all conditions, including off-normal events.

2. The necessary penetrations shall be provided.

3. The current port allocations for the vessel need to be discussed

4. The Vacuum Vessel support links the vessel to the magnet coil system. **I**t shall provide a reliable support for the weight of the Vacuum Vessel and all of its internal components in earthquake conditions. The support shall also resist horizontal and vertical forces from normal, off-normal events, and VDEs. It provides unrestrained

radial but restrained toroidal motion with reference to the TF coils.

5. The internal components of the VV shall have their vertical axis of symmetry coincident with the magnet axis, with tolerances as specified.

6. Drainage of the coolant in each sector will be necessary.

7. The Blanket supports shall accommodate VV to Blanket relative motion due to temperature conditions;

8. The vacuum vessel support structures shall accommodate the movement of the vessel in accordance with the space allocations.

9. Fabrication and assembly tolerances should be given.

Electrical Requirements

1. The toroidal electrical resistance of the VV shall be high enough to achieve initial plasma break down and current ramp up with acceptable loss of magnetic flux, and also allow the penetration of control magnetic field with acceptable damping effect.

2. Appropriate arrangement of all pipes and manifolds should be developed to restrict induced currents.

3. The VV shall be electrically insulated from the Magnet system to avoid shunting of designated grounding paths for TF coils and to break local eddy current loops.

4. The VV is connected electrically to the Cryostat via the metallic structures of all ports.

Nuclear Shielding Requirements

The vacuum vessel, blanket system, and divertor in combination must provide shielding for the superconducting coils. The blanket and divertor must provide shielding for the vessel to prevent unacceptable material damage and allow vessel rewelding.

Remote Maintenance Requirements

Specific remote handling requirements for the vacuum vessel and the end-effectors used to perform the remote cutting, welding, and inspection operations during sector replacement need to be considered.

Chemical Requirements

1. VV components must be compatible with the water coolant chemistry.

2. The water in the VV - PHTS must meet the following requirements: a. Low conductivity (Demineralized);b. Low O2 content

Seismic Requirements

The vacuum vessel will be designed to meet seismic design criteria adopted by the project that will establish the site specific characterisation of seismic events.

Manufacturing Requirements

1. The VV shall be manufactured consistent with an accepted code or standard.

2. Half sector tolerances must meet the following requirements:

3. After manufacturing is complete, the sector cooling channels and all inner and outer surfaces are to be flushed with a cleaning solution to remove oils and other residues, and then with pressurized water with detergent. After cleaning, the channels and surfaces are to be rinsed by demineralized water and then air dried.

4. All inner and outer surfaces of the vessel are to be cleaned with a solvent and then air dried.

5. Tests to be conducted during manufacturing

Construction Requirements

After the vessel components have been shipped to the construction site, they must be handled and stored as specified below:

1. The inner and outer surfaces of the vessel sector must be inspected for damage and contamination. Damage is to be reported and re-cleaning done if required.

2. Other vessel components are to be inventoried and stored in a clean dry enclosed area.

Assembly Requirements

1. Number of field joints must be minimised.

2. VV tolerances during assembly and of the completed torus must meet the following requirements

4.2 General structure design

4.2.1 The basic D shape for CFETR

The Figure 27gives the general structure dimension for the CFETR.

The general parameters about the VV are: the torus outer radius is 8.6 m, the inner torus radius is 2.6 m, the torus height is 9.7 m.

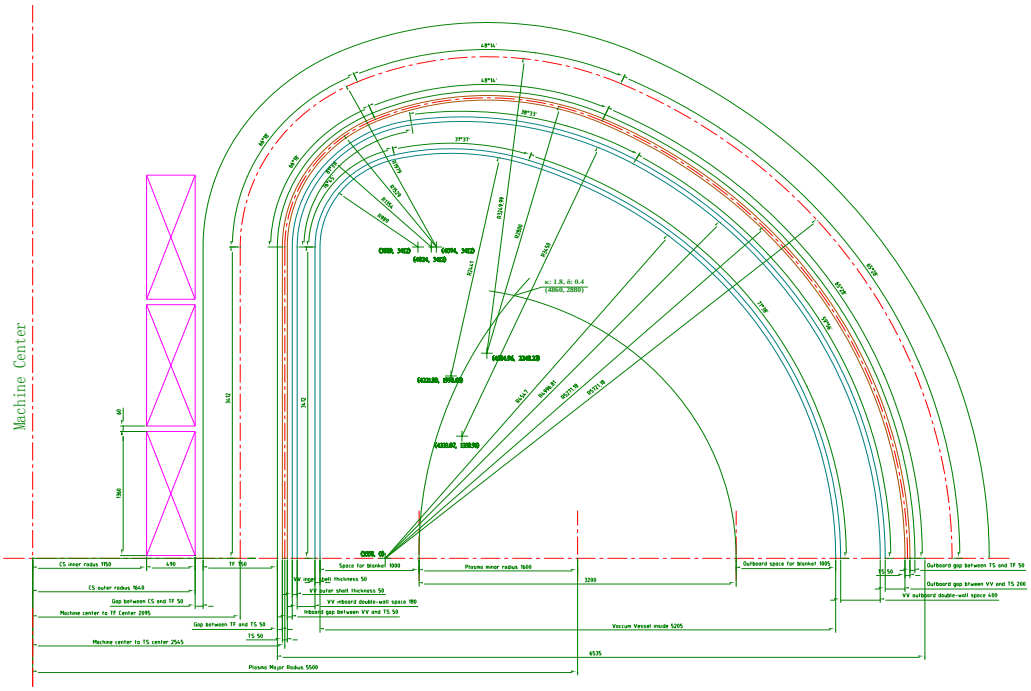

Figure 27 layout of the main components

According to this structure and dimension, the conceptual design for Vacuum Vessel is proposed by our design team.

2.2 The basic structure

The Figure 28 shows the basic design for CFETR VV. The basic structure is:

The quantity of upper ports and lower ports are both 12.

TheEquatorial ports are: 2 big ports which are used to remove the sectors and 10

normal sectors. The port layout is shown in the pictures below. The details for ports are shown in the table 23.

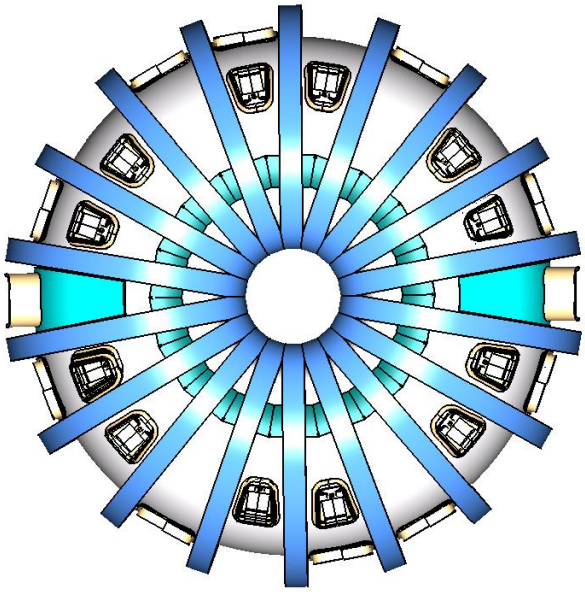

a

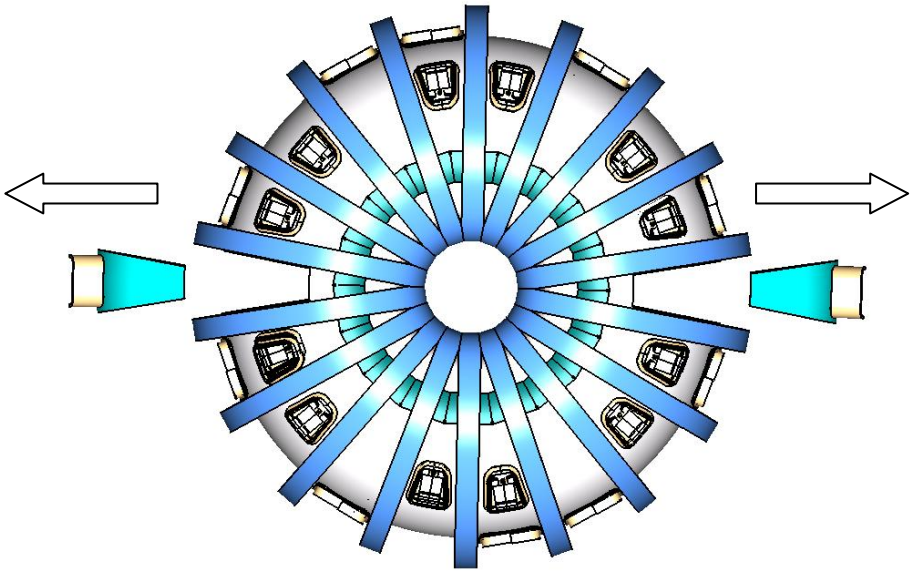

b

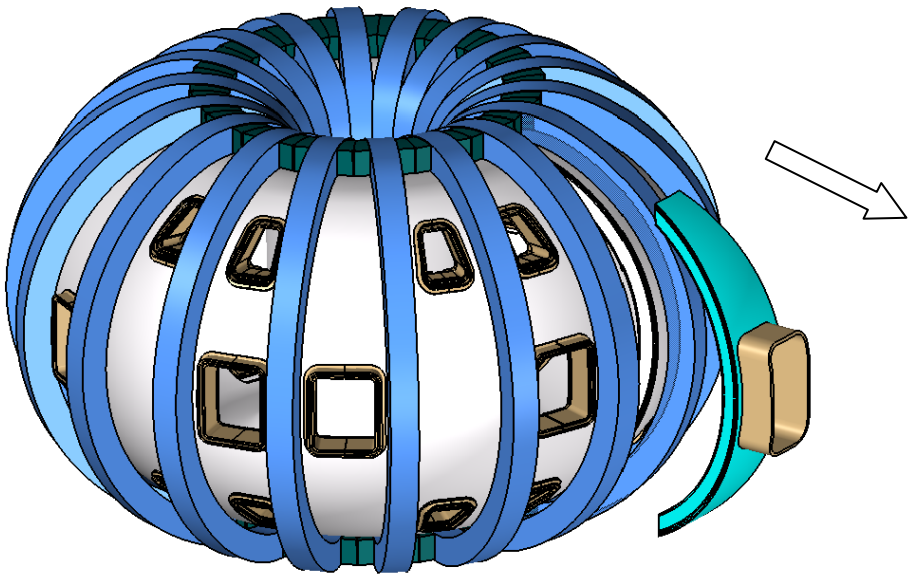

c

Figure 28 comparison of the ITER VV (left) and CFETR VV (right)

The figure 28 b and c show that the outboard of the two big port sectors can be removed integrally, for the assembly of other inner components .

This report will give a comparison between ITER VV and CFETR VV to show the new design structure.

Table 21 comparison between ITER VV and CFETR VV

	ITER VV	**CFETR VV***	
		Option 1	***Option2***
D shape (vertical direction)	Not symmetry	Symmetry	Symmetry
Ports (average in one sector)	5	3	3
Shell structure	Double shells	3 shells	Double shells with insulation layer
Radius space for VV	335-770(Two shells)	380-600(three	300-600(three

		shells)	shells)
Shell thickness	60mm	50mm	50mm
Housing structure	yes	no	no
Triangular support	yes	no	no
Big temperature difference	no	yes	yes

***Note: The following design is just for The *Option 1*; *Option 2* will be described in 4.3.**

2.2.1 The basic D shape for Vacuum Vessel

The ITER VV D shape is made up of about 7 arcs and 3 lines for inner shell, 6 arcs and 2 lines for out shell. The D shape is not symmetrical in vertical direction. Figure 29 shows the details.

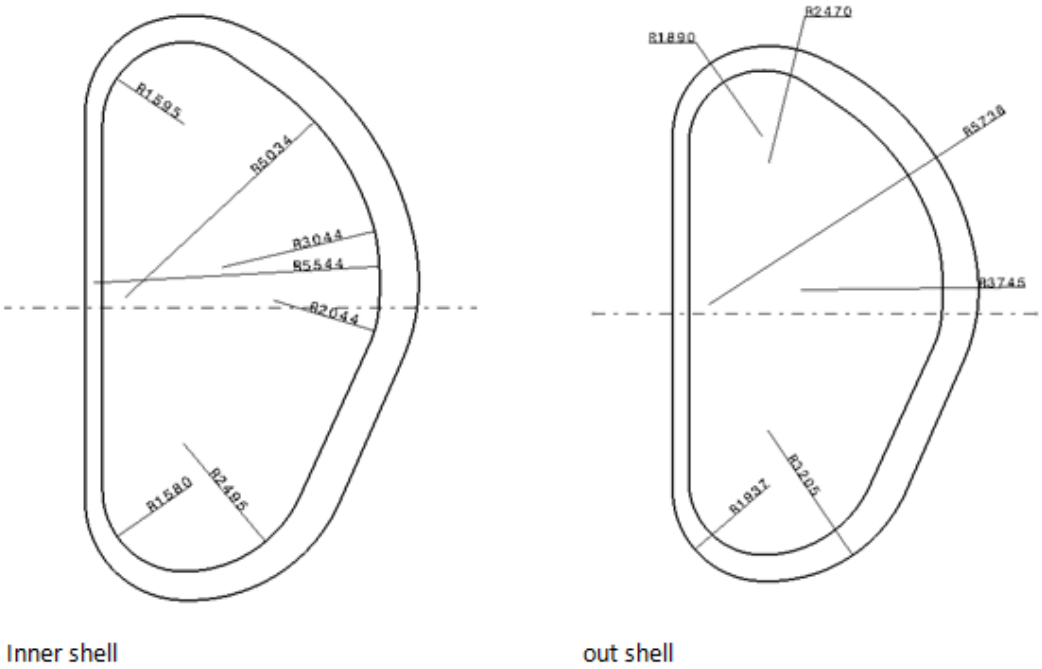

Figure 29ITER VV double shell dimensions

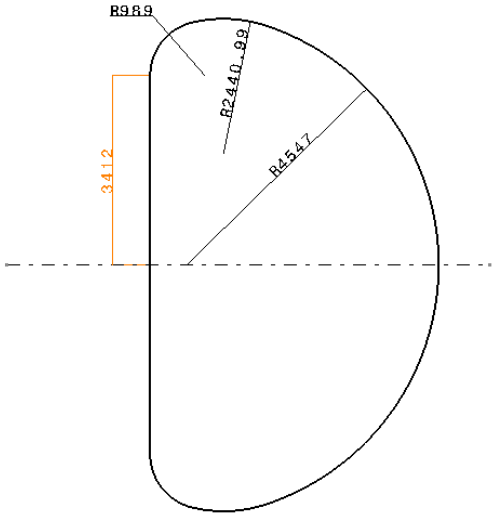

Figure 30 CFETR VV D shape

The D shape in CFETR VV is symmetrical in vertical direction for all three shells. This kind of D shape is made up of 5 arcs and 1 line for all shells. The Figure 30 gives the basic dimension for the structure of inner shell.

By comparing between these two shapes, it is obvious that the CFETR VV is easier to design and manufacture. And this shape can be verified by the theoretical calculation and analysis simulation.

2.2.2 The port layout

Considering the purpose of CFETR, the basic layout for port is established as Figure 31 shows.

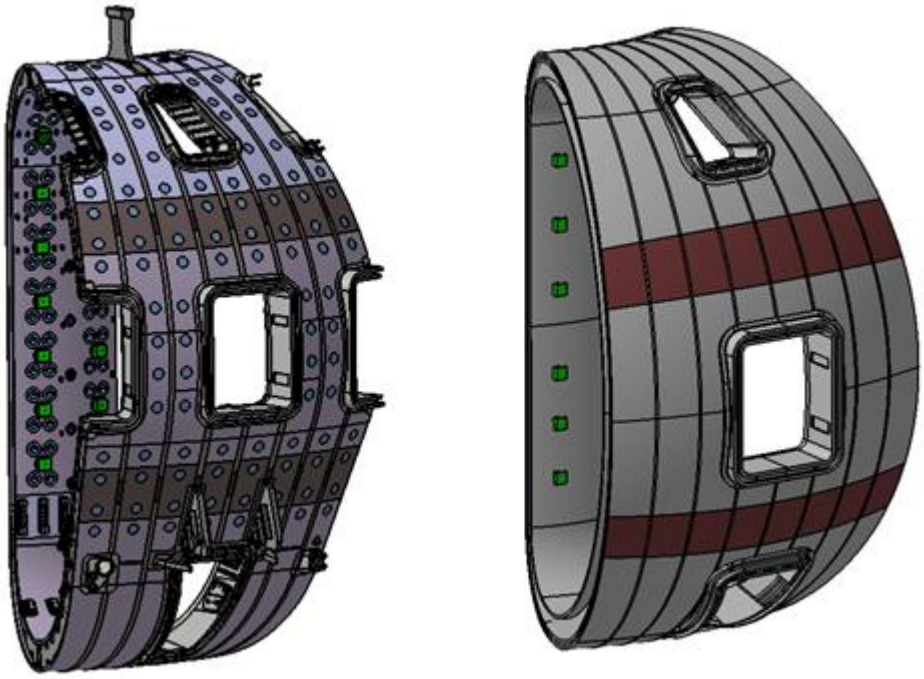

Figure 31 port comparison (ITER VV: left, CFETR VV: right)

The ITER is a great experimental reactor, it would be used for many kinds of experimental test, so many ports are necessary for different kinds of function.

The planned-function for the ports is listed in Table 22:

Table 22 ITER VV ports quantity and function

Port Type	Quantity	Function
Upper	18	Diagnostics , EC Systems, VV/Blanket piping
Equatorial	14	Regular (RH/ Port Limiter, RH Heating Systems, Diagnostics, Test Blanket modules)
	2	Heating Neutral Beam
	1	Heating/ Diagnostics Neutral Beam
Lower	4	RH/ Diagnostics, VV/ Divertor piping
	5	Cryopumps
	18	Local penetrations (IVV/GDC Systems, Divertor piping, VS coil feeders)

The CFETR is a great experimental reactor, but for commercial purpose. So the functional ports can be reduced to the minimum to satisfy the operating request, as Table 23 shows.

Table 23 CFETR VV ports quantity and function

Port Type	**Quantity**	**Function**
Upper	12	Diagnostics (5) ,Divertors(5), VV/Blanket piping(2)
Equatorial	8	LHCD(1), ECRH(1),Diagnostics(3-4),VV/Blanket piping(2)
	2	Heating Neutral Beam
	2 Big port	Sector removing
Lower	12	Diagnostics (5) ,Divertors(5), VV/Blanket piping(2)

Also another option for port layout is taken into count now. (Shown in Figure 32)

This conceptual design is to use the big port to assembly the inner model (robot hand). And the detail design will add some penetration for the cooling system and other function.

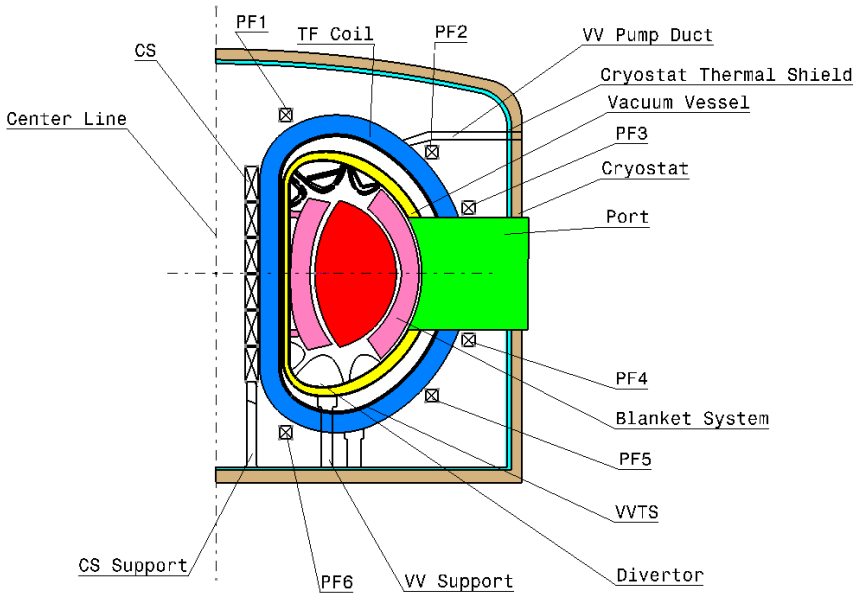

Figure 32 alternative port design

2.2.3 The rib layout

The ITER rib-layout is: supporting ribs with housings (the highlight in Figure 33). Considering the complex structure of ITER rib-layout and the difficulty of manufacture for housing and the too much welding between rib and housing, our design gives up the housing structure.

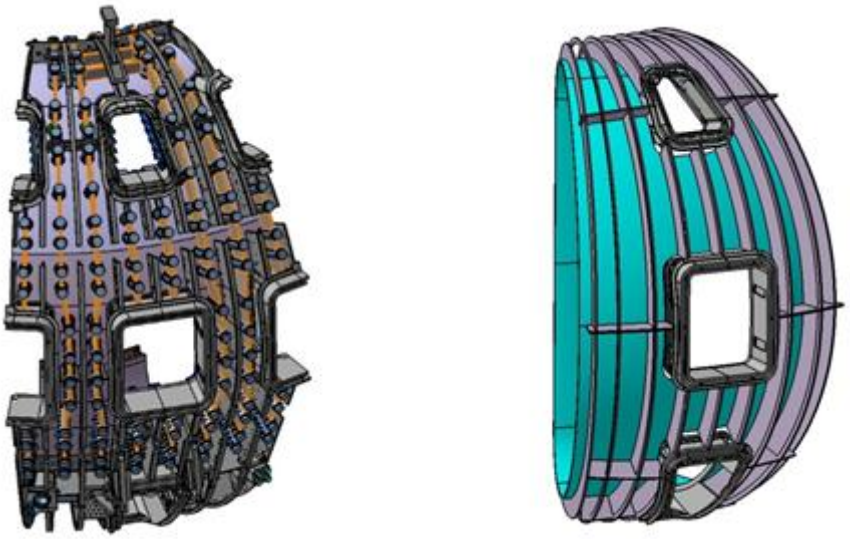

Figure 33 reinforcement rib comparison (ITER VV: left, CFETR VV: right)

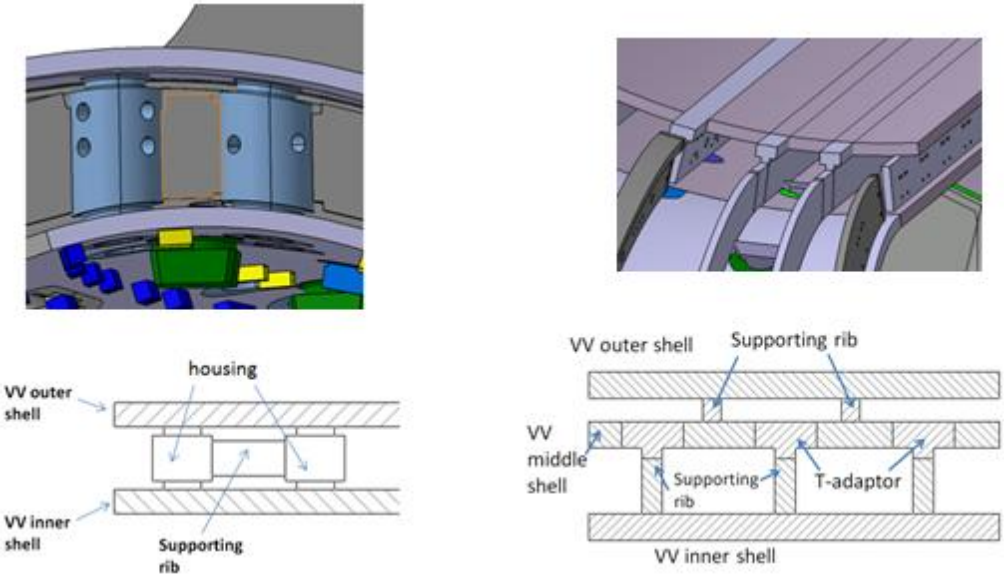

Figure 34 in-wall support structure comparison (ITER VV: left, CFETR VV: right)

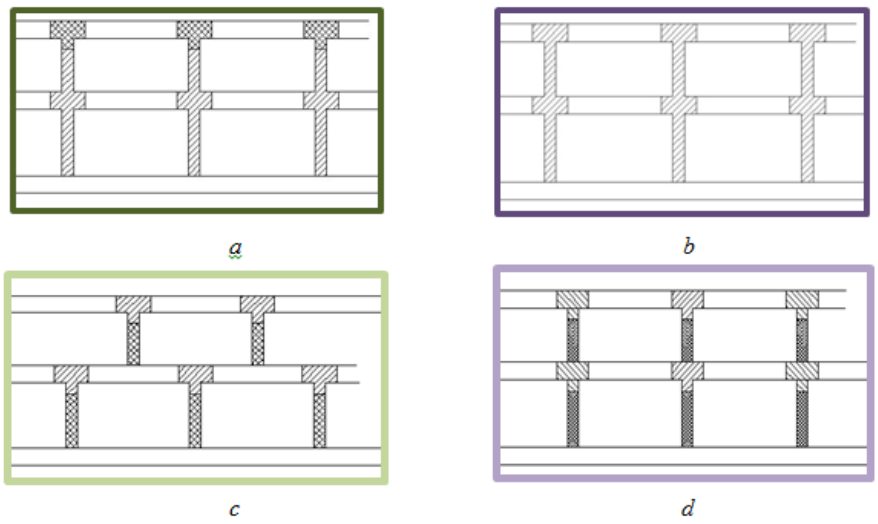

Figure 35 four candidate connection designs for the three shells

The option a is : use the cruciform-shape rib and T-shape adaptor

The option b is : use one rib to reduce the length of welding line

The option c and d are both use the T-shape rib same to ITER T-rib structure.

These ribs-structure will be verified by kinds of analysis simulation.

2.2.4 The triangular support optimization

By considering the complex of the triangular, we decide to simplify this structure. After the several discussions in our design team and refer to the design from other project like Dr. Rebut's idea, the triangular support structure is replaced by several big supporting keys. (The triangular support is a structure which supports the blanket to add the plasma vertical stability. It is a complex structure with a part attached to the VV and a complex removable part.) This key-structure also can simplify the cooling structure because ITER triangular support should be cooled by cooling structure.

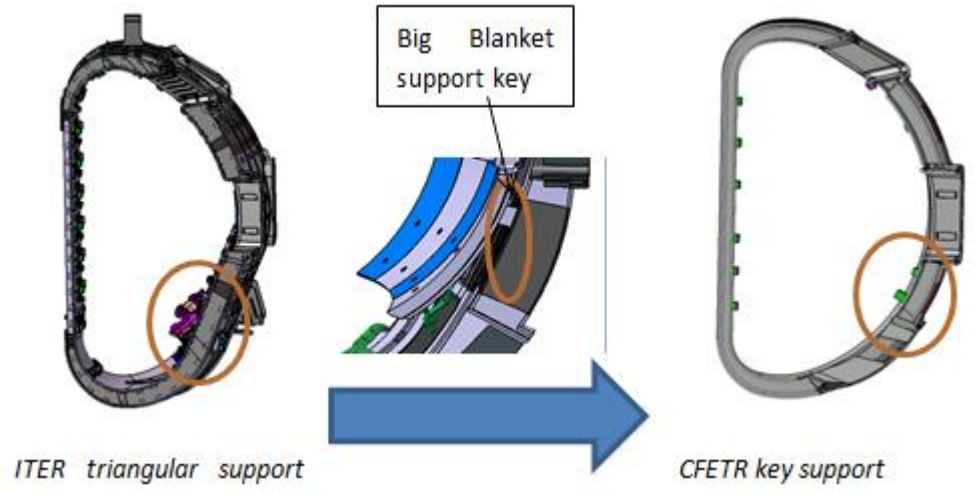

Figure 36 change of the triangle blanket support

1. The cooling flow structure design

As we know that the cooling flow of ITER VV is with two loops cooling flow for each 20 °sub-sector (one loop from lower port to upper port, through inboard area; the other one is also from lower port to upper port, but through outboard), through the two shells of Vacuum Vessel. This cooling flow structure can achieve the big temperature difference. So our VV conceptual design is three-shells-structure (the space between the middle shell and the third (outer) shell is for the cooling flow. The details are shown in Figure 37. Two loops cooling flow are also applied.

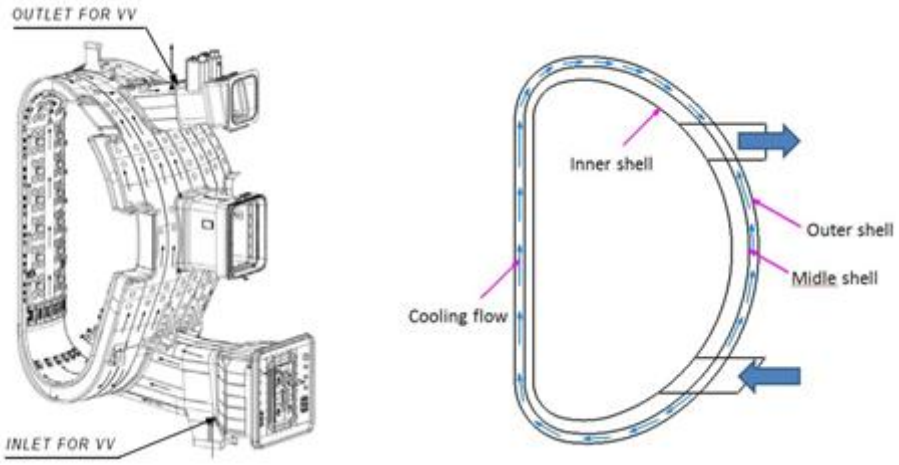

Figure 37 cooling loop comparison (ITER VV: left, CFETR VV: right)

4.3 Thermal analysis

4.3.1 Analysis assumption

The temperature of VV will be very high by the impact of the αlphaparticle and neutron from the plasma, mostly the impact of the volumetric heat of the Neutron deposition.

The ITER and EAST have water cooling vacuum vessel to control the VV temperature at 100 ℃ on both shells. The water enters at the bottom of the VV, fills the gap between the two shells and leaves on the top.

In the CFETR, this cooling method is kept to eliminate the nuclear heat, but in order to reduce the tritium deposition, the inner wall temperature should be kept above 500℃, then the radiation heat load to the 80K VVTS will increase by 18 times, which should be reduced to save cryogenic cooling power of the thermal shield system, thus there is another design target to control the outer VV surface temperature below 100℃.

The analysis is done on a simplified VV model, which includes the shells and ribs of the lower half of 40 °VV , in order to check the thermal performance of the main body, the ports and water entrance & exit are not included because they won't have much impact on the section temperature distribution.

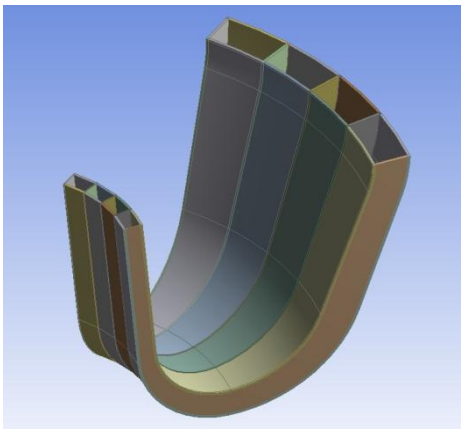

Figure 38 VV analysis model

4.3.2 Loads and boundary conditions

According to the ITER specification, the maximum nuclear heating rate is 0.4MW/m^3 on the VV, and the distribution is not uniform, like Figure 39shows, the crossroad of uncovered surfaces has the peak heat generation rate, as well as the temperature. Meanwhile, due to the distance rise and the shielding of the In-wall blocks, the neutron impact on the outer shell is much reduced than the inner one, therefore in the analysis, only inner wall has a uniform internal heat generation of 0.4 MW/m^3 to be conservative.

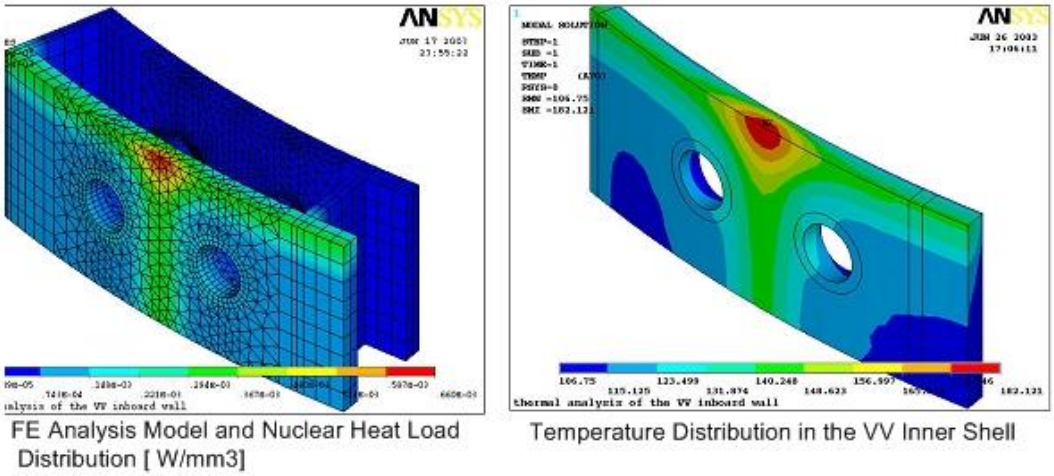

Figure 39 nuclear heat and temperature distribution on the ITER vacuum vessel

Because the VV coolant channel doesn't have a constant section along the flow path, which brings in changing convection calculations, thus the FSI (fluid-solid interface) between the water and the wall is simplified into a wall temperature which is equal to the water.

The blanket and other internal components which face the inner shell are considered to have similar temperature with the hot wall; therefore the radiation in this direction is ignored. However, the radiation between the outer shell and the VVTS is considered.

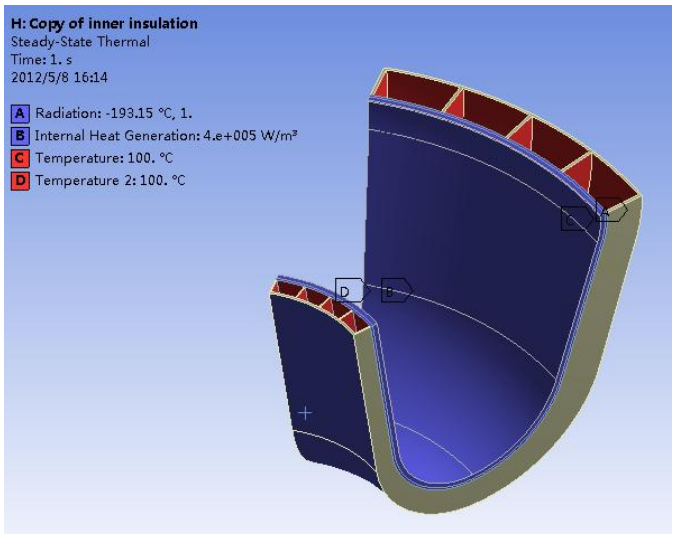

Figure 40 VV analysis loads and BC

4.3.3 Three-shell design results

This design adds an additional shell inside the inner shell, which doesn't have direct cooling like the basic two shells, and therefore it isn't required to be air tight, and there should be openings to ease the vacuum pumping.

This analysis employs the model in Figure 41, and the radiation between the additional shell and the inner shell is an important cooling method, especially there is a huge temperature difference between these two shells.

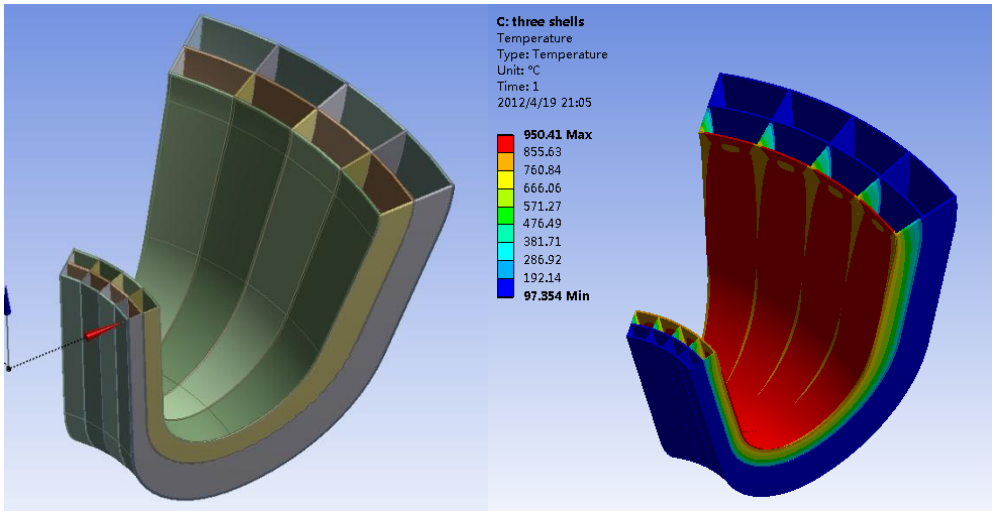

Figure 41 three shell model and temperature distribution

In this model, the temperature on the additional shell is 950℃, which already exceeds the requirement, reducing the conduction resistance between the additional shell and the inner one can control the temperature by shortening the rib between them or adding thermal connectors.

4.3.4 Other design discussion

Besides the three-shell design, there are two designs which could meet the 500-100℃ operation requirement, one is water cooling vacuum vessel with inner insulation layer, the other is helium cooling vacuum vessel with outer insulation layer. Both of them have only two shells, and reduce the difficulty of manufacture and space requirement.

4.4.1 Water cooling VV with inner insulation

This design uses normal cooling double-shell configuration at 100℃, and an insulation layer is placed inside the inner shell to provide needed thermal resistance.

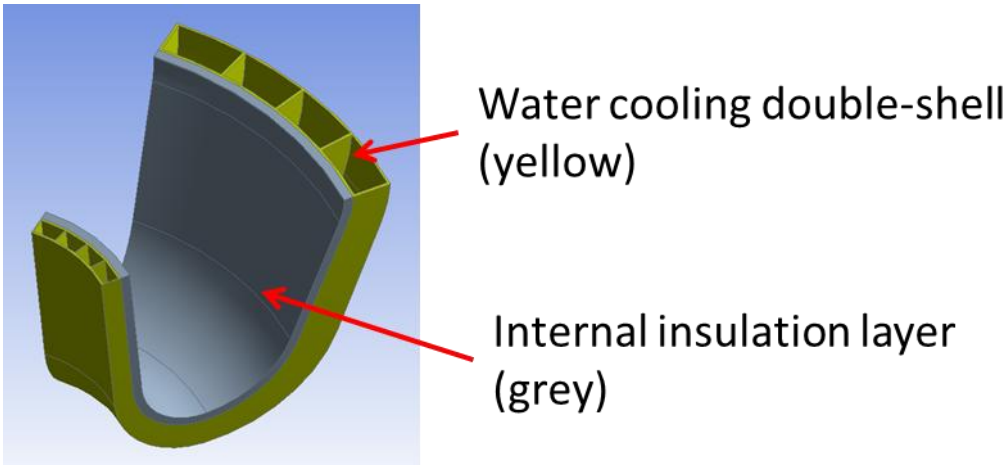

Figure 42 inner insulation design

To get 500℃ on the inner surface of the insulation layer, the thickness is increased to achieve enough resistance, Figure 43 is the relationship between peak temperature and thickness.

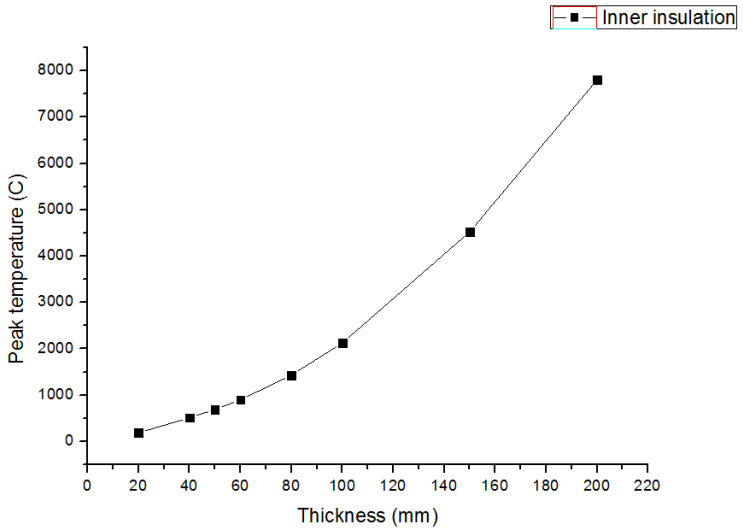

Figure 43 peak temperature vs. insulation thickness

The insulation layer increases the distance between the blanket and the inner shell, and this enlarge the load on the blanket support, so the insulation layer should be as compact as possible, which requires low conductivity. Figure 44 gives the relationship, the thickness is constraint to 20mm.

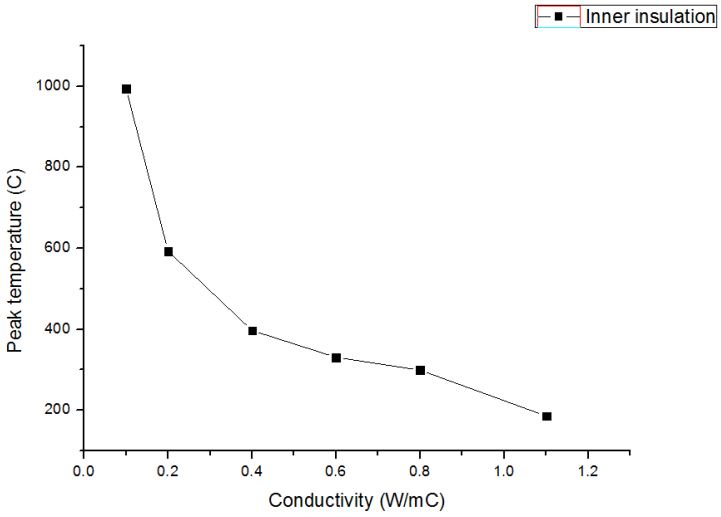

Figure 44 peak temperature vs. insulation conductivity

According to Figure 44, a thermal conductivity of 0.3W/m℃ is required.

4.4.2 Helium cooling VV with outer insulation

The insulation layer is a new material and its performance under neutron radiation is unknown, thus the inner insulation design has some uncertainty; and a high temperature VV with outer insulation design is proposed, like Figure 45, the difference is that the insulation layer is placed outside the double-shell.

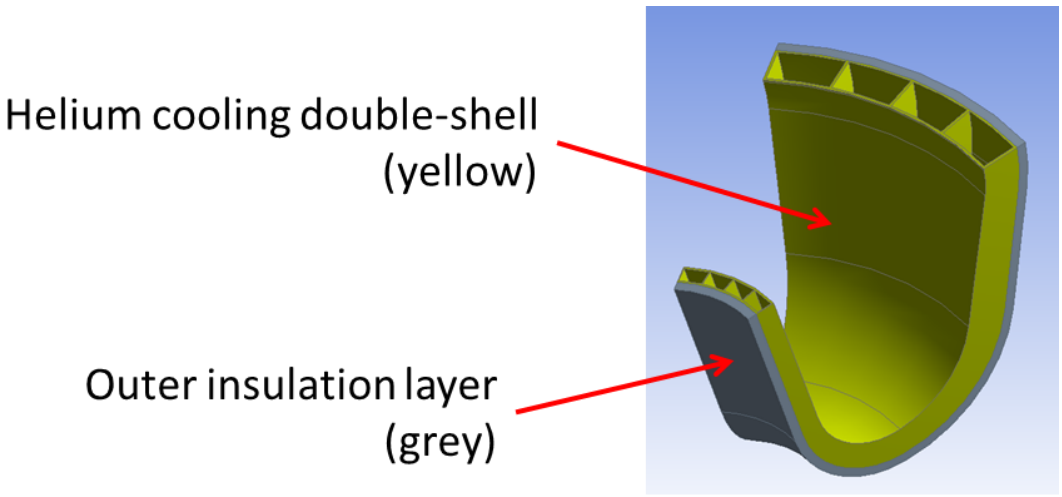

Figure 45 outer insulation design

In this design, the VV main body works at 500℃, and the insulation should reduce the outer surface temperature to 100℃ to minimize the heat load to the VVTS.

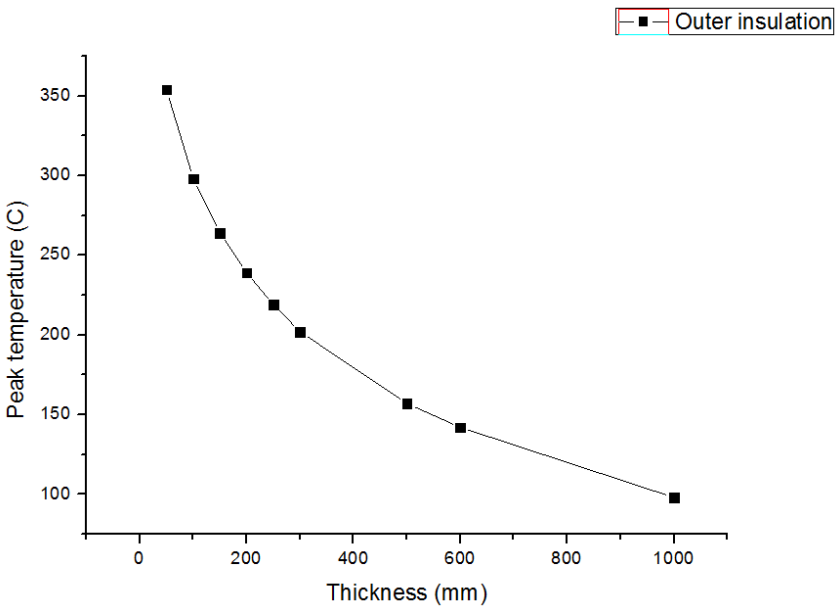

Figure 46 peak temperature vs. insulation thickness

According to Figure 46, to produce the 400℃ temperature difference, 1000mm thick insulation layer is asked for, which is impossible to realize, and this indicates the efficiency of the outer insulation is lower than the inner one.

If the thickness is also constraint to 20mm, and a temperature-conductivity curve can be drawn in Figure 47. Compared to the 0.3W/m℃, the requirement rises to 0.02W/m℃, which is more difficult to get. Meanwhile, this plan asks for high temperature base material like engine steel and helium cooling system, which also bring problems.

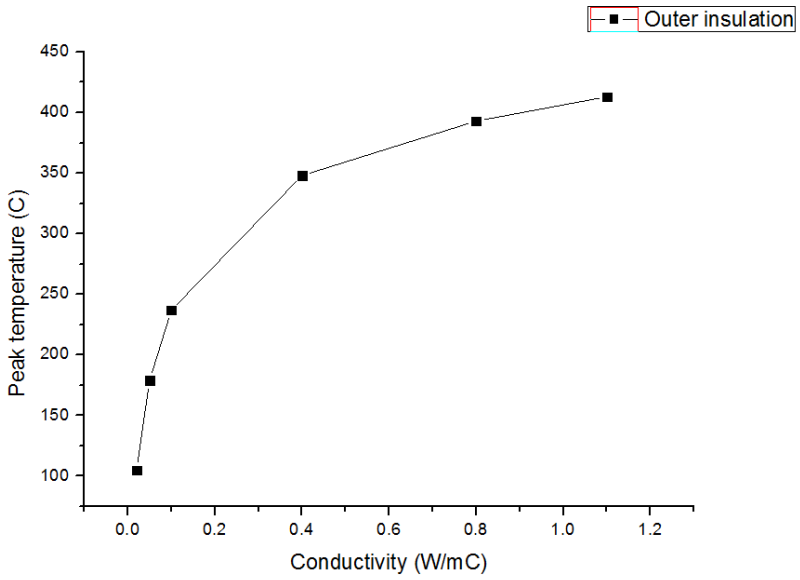

Figure 47 peak temperature vs. insulation conductivity

4.3.5 Summary and Future Work Plan

The most important difference between the CFETR VV and the ITER is hot-wall operation, and three candidate designs are proposed. The three-shell design can refer to the long-term experience of double-shell VV, and the material choice is mature, but the space and manufacture requirement is high; the inner insulation design can compensate these disadvantages, but the R&D work of the insulation material is a new task; the outer insulation design simplifies the insulation working environment, but the requirement to the thermal conductivity is higher, there are also problems on the high temperature steel and helium cooling system.

Up to now, all the works are for the conceptual design. The future works are: Firstly, we need to do the material R&D to decide the design option. Then the detail design, the assembly simulation, the structure analysis, the thermal analysis and all optimization works should be considered.

5 Thermal shield

5.1 System description

5.1.1 System Functions

The CFETR Thermal Shield has the following system functions:

1. The thermal shield system provides an effective optically opaque barrier for total and local thermal loads from the warm components to the superconducting magnet that maintain at 4.5K, whether by thermal radiation or conduction, during normal operation, and during vacuum vessel baking.
2. The thermal shield system shall provide an acceptably low thermal radiation emissivity so that the heat loads to the 80K thermal shield and 4.5K magnet systems can be handled cost effectively by the cryogenics plant.
3. It shall provide access ports for in-cryostat components, maintenance equipment and diagnostics.
4. The design basis conditions include all credible combinations of loads, seismic loads, electromagnetic loads, and pressure loads.
5. The operating pressure and pressure drops shall be compatible with the cryoplant warm compressors.
6. The thermal shield system shall have suitable instrumentation to monitor the TS status and provide confidence that the system requirements are met during all modes of operation.
7. It is the system responsible for the overall neutron shielding of the TFC and provide reliable operation with better than 99.9% reliability.

5.1.2 Basic Configuration

The thermal shields shall form an optically opaque reflector (barrier) between all warm surfaces (at room temperature, and above) that have the potential for emitting thermal radiation to the supercritical helium temperature magnet structures.

All TS components shall be equipped with cooling pipes that are attached to its surfaces.

The cooling pipes shall be connected to the manifolds, and the manifolds shall be routed to the cold valve boxes installed in outside of the bio-shield.

There shall be labyrinth interfaces at the boundary areas of the components of the TS that prevent a direct shine-through of the warm surfaces to the cold ones and allow vacuum pumping.

5.2 2 System Design Requirements

5.2.1 General requirements

The thermal shield shall satisfy the upper limit for both total and local thermal loads, applied to the surfaces of components operating at 4.5K, by thermal radiation and/or conduction.

At normal plasma operation conditions, the thermal loads from the thermal shield to the surfaces at 4.5 K shall be limited to 2.2 kW, which includes the thermal radiation and thermal conduction through the thermal shield supports. Thermal load from 80 K to 4.5 K in the magnet gravity support is not included.

In addition, the maximum surface heat loads on the 4.5K surfaces shall be limited to 40 W/m2 locally, provided the above totals are not exceeded.

The thermal loads on the TS at 80K shall be below approximately 300 kW during plasma operation state, and approximately 500 kW during a baking operation state.

5.2.2 System specific requirements

Thermal radiation to the superconducting magnets shall be minimized by operating the thermal shields at temperature of 80-100K and providing surfaces with low emissivity (for example, with an average value of 0.05 at 80K).

The coolant for normal operation shall be pressurized He gas with an 80K nominal inlet temperature.

The operating pressure and pressure drops shall be compatible with the cryoplant warm compressors.

The inlet pressure inside the cooling pipes shall be 1.8 MPa.

The design pressure inside the cooling pipes shall be 2.1 MPa.

During the normal plasma operation, the overall pressure drop on each thermal shield cooling line (comprising of cooling tube attached on the TS panel and helium manifold) shall be less than 0.1 MPa.

The thermal shield and thermal anchors shall be designed to remove the heat due to:

- ✧ The thermal radiation from the VV, with VV surface emissivity, which shall be about 0.35, and whose temperature shall be 120C (during normal operation) and 200C (during VV baking).
- ✧ The radiation and conduction through the CTS supports from the cryostat at room temperature.
- ✧ The radiation from the VV manifolds, whose temperature shall be 120C (during normal operation) and 200C (during VV baking).
- ✧ The radiation from the blanket manifolds, whose temperature shall be up to 150C (during normal operation) and up to 250C (during VV baking).
- ✧ The nuclear heating, which shall be maximum 400 W/m3 in inboard of VVTS.

It is foreseen that advance cool-down of magnets, with a temperature difference of 75C between TS and magnet inlet temperatures, shall be performed.

Mechanical requirements

The TS components in the assembled state and their sub-components shall withstand, without incurring damage that requires repair, all loads (gravity, thermal and electromagnetic), deflection of supporting components (such as the TF coils), loads that are experienced during assembly and disassembly, tests, seismic events and off-normal events.

All thermal shields shall allow thermal expansion/contraction without excessive stress. Clearances shall be sufficient for the maximum design thermal deflections.

Other requirements

Seismic requirements: All thermal shields shall be designed to withstand the seismic loads that can affect the TS components.

Fire protection requirements: None of the components of the thermal shields shall be flammable.

Vacuum requirements: The structural materials to be used shall be consistent with providing a high quality vacuum. The maximum allowable leak rate for the TS assembly shall be 1 x 10-5 Pam3/s.

Thermal management requirements: The TS shall remove the heat transferred from the VV and Cryostat.

Electromagnetic requirements: The TS shall have a number of electrical breaks to reduce the induced currents to a level that avoids a complication of the TS design from the electromagnetic loading context. The electrical resistance of the thermal shield shall be large enough so as not to perturb the poloidal field system.

Nuclear shielding requirements: As a component placed between the VV and TFC, the VVTS shall be taken into account for the overall neutron shielding of the TFC.

Materials requirements: The thermal shield materials and surface finishing shall be compatible with the requirements of the Vacuum Handbook. The materials shall be also selected considering cost, performance and manufacturing. The surface of TS facing other components shall be coated with a low emissivity material. Structural material with low thermal conductivity and high strength shall be used for the supports.

Non-metallic materials may be used for electrical insulation, and low heat loss structural components. These materials shall be compatible with the nuclear environment at the thermal shields.

Assembly requirements: The overall TS assembly and assembly of the individual sub-components shall be compatible with assembly of VV, TF and PF coils, and other components of the CFETR-machine. The on-site assembly activities shall be integrated with the overall machine assembly schedule.

Installation requirements: The TS shall be installed in accordance with the overall machine assembly procedure.

5.3 Conceptual Design Descriptions

CFETR thermal shield is located outside the vacuum vessel and inside cryostat. It is a single wall structure primarily fabricated with 304 stainless steel and 80 K helium flows in cooling pipes/channels that are permanently attached to the wall. It operates inside cryostat vacuum environment. The thermal shields system shall consist of Vacuum vessel thermal shield, Cryostat thermal shield and Support thermal shield. The cryostat thermal shield consists of the upper cryostat thermal shield, equatorial cryostat thermal shield and lower cryostat thermal shield. Equatorial thermal shield consists of the vacuum vessel thermal shield and equatorial cryostat thermal shield.

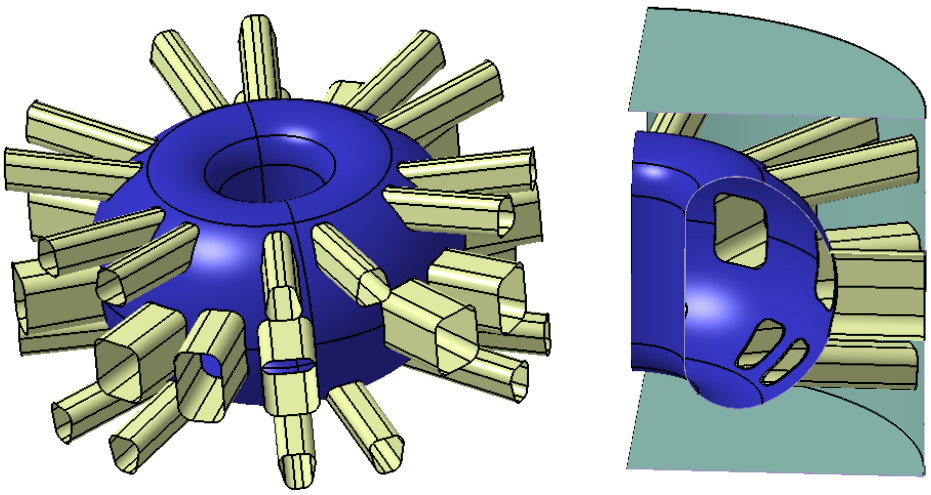

Figure 48 main components of the thermal shield

The cryostat thermal shield is mounted alongside the walls of the cryostat (bottom, cylinder and top head), thereby preventing direct line of sight from the room temperature cryostat walls to the cold components of the CFETR. The port thermal shields that enclose the port connecting ducts are routed between the cryostat walls and the vacuum vessel. The support thermal shields enwrap the vacuum vessel gravity supports and machine gravity supports. The support thermal shields thermal anchors in the vacuum vessel and machine supports limit the heat load to cold structures due to conduction through the support structures.

The vacuum vessel thermal shield has about1, 900 m2, and surface area, slightly higher than the vacuum vessel radiating area. The cryostat thermal shield and support thermal shield have an area about 3,000 m2.

5.3.1 Cryostat Thermal Shield

The cryostat thermal shield consists of the upper cryostat thermal shield lid, the cryostat thermal shield cylinder and the lower cryostat thermal shield floor. The upper cryostat thermal shield lid is supported from mounts off the cryostat lid. The cooling tubes will be welded on the inside surface of the cryostat thermal shield for the accessibility of tube connection.

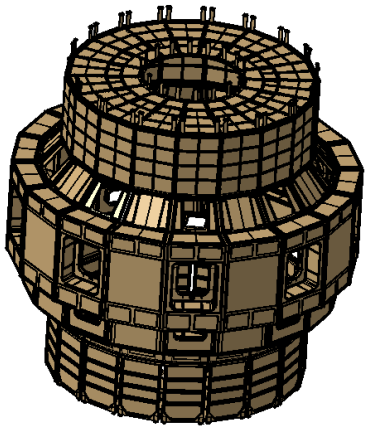

Figure 49cryostat thermal shield

The design of the cryostat thermal shield is based on a self-standing concept: thick stainless steel panels which are reinforced by an extruded member and attached to the neighbouring components of the cryostat with the help of Ti-alloy supports. Panel frames of the cryostat thermal shield are interconnected by splice plate bolted joints to form a self standing cylinder of thermal shield components. The primary function of the cryostat thermal shield is to shield the superconducting magnets from heat radiating from the inner wall of the cryostat.

5.3.2 Vacuum Vessel Thermal Shield

The vacuum vessel thermal shield is interposed between the VV and the cold magnet structures. The vacuum vessel thermal shield is a continuous self-standing screen surrounding the outer surface of the vacuum vessel and its ports. The vacuum vessel thermal shield has toroidal and poloidal electrical breaks in order to reduce induced electro-magnetic loads. The positions of these electrical breaks coincide with sub-assembly and assembly joints. The poloidal breaks divide the vacuum vessel thermal shield into inboard and outboard parts.

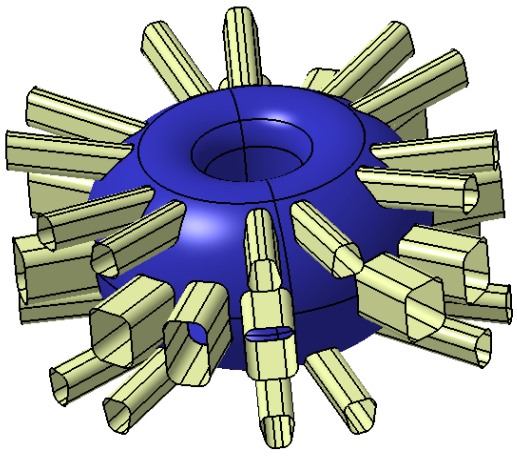

Figure 50Thevacuum vessel thermal shield

5.3.3 Interfaces

The thermal shield system shall have:

- ✧ Connections to the TF coils, via the equatorial thermal shield supports.
- ✧ Functional interfaces with all warm components of CFETR tokamak. It is facing to, namely - with the Vacuum Vessel including the port structures, the Cryostat, the Cooling Water System.
- ✧ Functional interfaces with the cold components, namely - the Magnets including all sub-components the thermal shield is also facing to.
- ✧ Functional interface with vacuum pumping system.
- ✧ Functional and physical interface with machine assembly and tooling.
- ✧ Connections to the cryostat, via the upper/lower cryostat TS supports.
- ✧ Connections to the magnet gravity supports, via the joints between the manifolds belonging to the thermal shield and Magnet system.

5.4 Primary heat load calculation of CFETR thermal shield

5.4.1 Load Types

The thermal loads acting on the thermal shield can be described as :

Thermal radiation on the thermal shield surface

Thermal conduction through the thermal shield supports

Heat transfer by convection

Neutron heating in the thermal shield components (volumetric)

NOTE: Neutron heating and thermal conduction through the thermal shield supports do not calculate, because the specific parameters cannot confirm now.

5.4.2 Heat Loads into the Thermal Shield

Thermal radiation is calculated using Kirchhoff’s law of thermal radiation:

$$Q = \frac{\sigma\left(T_h^4 - T_c^4\right)A}{\left(\frac{1}{\varepsilon_1} + \frac{1}{\varepsilon_2} - 1\right)}$$

where：

σ - Stefan - Boltzman constant ($5.67 \times 10^{-8} W.m^{-2}.K^{-4}$)

T_h – hot surface temperature (K)

T_c - cold surface temperature (K)

A - surface area exposed to radiation (m^2)

ε_1 - emissivity of surface 1

ε_2 - emissivity of surface 2

The emissivity of various surfaces is defined in Table 24:

Table 24 emissivity of different components*

Vacuum vessel and ports surface	0.35
Cryostat surface	0.5
Thermal shield surface	0.06

* The emissivity refer to ITER components emissivity

The temperatures of the various components radiating heat onto the thermal shield are defined in Table 25 during plasma operation state and vacuum vessel baking operation state:

Table 25 component temperature

Components	Plasma operation state	Baking operation state
Vacuum vessel	393	473
Cryostat	300	300
thermal shield	80	80

Thermal radiation into thermal shield is calculated, and listed in Table 26.

Table 26 radiation heat load to the VVTS from the VV

Plasma operation state	~216KW
Baking operation state	~369KW

Heat transfer by convection is calculated by Eq.1

$$Q = \wedge \cdot p \frac{\alpha}{2-\alpha}\left(T_2 - T_1\right)S \quad \text{W} \qquad (1)$$

$$\wedge = \frac{1}{2}\left(\frac{\gamma+1}{\gamma-1}\right)\sqrt{\frac{R}{2\pi MT}} = 5.752\times10^{-1}\left(\frac{\gamma+1}{\gamma-1}\right)\sqrt{\frac{1}{MT}} \quad \text{m/K•s} \qquad (2)$$

Where:

$\wedge$ - Free molecular thermal conductivity

M – Gas molar mass

γ - Adiabatic exponent

T – Temperature

R - molar gas constant, 8.314J/(mol•K)

S – Area

p- Gas Pressure (1×10^{-5}Pa)

α - Adaptation coefficient

Heat transfer by convection is calculated, and listed in Table 27.

Table 27 convection heat transfer

Plasma operation state	~9.5W
Baking operation state	~10.9W

5.4.3 Heat Loads from the Thermal Shield

Thermal radiation is calculated using Kirchhoff's law of thermal radiation. The magnet

is analysed as a black body due to the formation of ice crystals on the outer surfaces. The effective temperature of the thermal shield is taken as100K during plasma operation state. The heat load form the thermal shield is about 1.7KW.

5.5 Conclusions

- The heat loads into the thermal shield are below the design requirements during plasma operation state and baking operation state.
- If the cooling system of the thermal shield can meet the effective temperature below 100K, the thermal loads from the thermal shield can also satisfy the design requirements.

5.6 CFETR thermal shield surface treatment alternative schemes

Thermal shield and vacuum vessel surface treatment alternative schemes are listed in Table 28.

Table 28 alternative design schemes

Design scheme	Warm surface temperature，Emissivity	Cold surface temperature，Emissivity	Heat Flux W/m2
No heat insulation layer No coating layer	373K,0.3	80K,0.3	193
No heat insulation layer Thermal shield silver coated	373K,0.3	80K,0.03	31
Thermal shield heat insulation layer	373K,0.3	99K,0.3	193

No coating layer			
Thermal shield, vacuum vessel heat insulation layer No coating layer	372K,0.3	81K,0.3	191

*Insulation thickness is 5mm; the thermal conductivity of heat insulation layer 1W/m℃.

From the Table 28, it can be seen that all the alternative design schemes has similar heat flux except the thermal shield silver-coated scheme , because the thermal resistance of heat insulation compared to radiation thermal resistance is too small. The thermal conductivity is the key parameter without increasing the thickness insulation layer. Figure 51 illustrated comparative analyses of scheme 4, and the radiation heat load acting on thermal shield will have obvious decrease until the thermal conductivity below 0.1W/m℃.

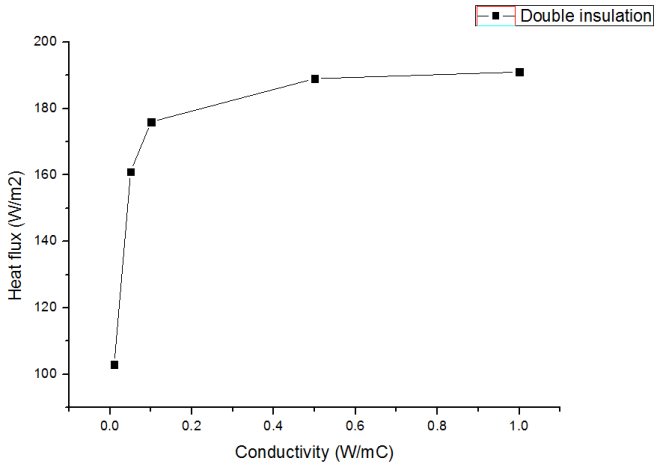

Figure 51 radiation heat flux between the VV and the VVTS vs. insulation conductivity

6 Cryostat

6.1 System description

6.1.1 Basic functions

- CFETR cryostat forms a vacuum tight container, surrounding the entire Tokamak basic machine. It provides the vacuum insulation environment to avoid excessive thermal loads (conduction and convection) from being applied to the components that are operated at cryogenic temperatures, such as superconducting magnet systems, thermal shields etc.
- Cryostat transfers all the loads that derive from the Tokamak basic machine, including the cryostatitself, to the floor of the Tokamak pit through its support structures.
- The port penetrations shall be connected to vacuum vessel (VV) port ducts and bio-shield port cells by metallic bellows to compensate all relative movements during the normal and off-normal operational regimes and at specified accidental conditions. These bellows system design shall also meet relative movements requirements between the as built and operation states.

6.1.2 Basic configurations

- The cryostat shall be a cylindrical VV, with its axis vertical, and with a flat bottom head & a tori-spherical top lid. The pedestal ring shall be theplatform to cater for the Magnets and the Vacuum Vessel supports.
- The pedestal ring shall be supported by 18 columns installed on the pit floor and by the skirt support.
- The skirt support shall allow radial movement of the cryostat shell in case of Helium and water spillage event inside the cryostat. The radial support lugs, which

are installed on the outer periphery of cryostat and are installed on bio-shield wall, shall confine the cryostat and the Tokamak basic machine fromhorizontal movement during seismic events.

- The cryostat shall be provided with removable central cover in top lid, in case of possible removal of Central solenoid (CS)coils.
- The cryostat flat bottom shall have provision of central welded cover to support initial assembly.
- The cryostat shall be connected with a means for draining to release the water after ingress of coolant event (ICE) inside cryostat.
- The cryostat shall have all necessary instruments for operation, monitoring and control information.

6.2 System design requirements

6.2.1 General requirements

- The Cryostat shall provide a reliable structural integrity and vacuum boundary for the life time of CFTERexperiment: Fatigue life for a minimum of 100 no. of vacuum pump down in a CFTER operation life
- The Cryostat shall be designed and manufactured using reference code: ASME section VIII-Div.2.
- The design internal pressure for the cryostat: 0.11 MPa, & 0.2 MPa, while the external pressure for operating conditions: 0.10 MPa.
- The connections between cryostat penetrations and the vacuum vessel port extensions shall incorporateport duct bellows to accommodate mutual thermal expansions and movements during operation, and during abnormal events this bellow system shall also accommodate the as built movement.
- The port cell bellows shall be included between the cryostat penetrations and port cells to compensate for cryostat movement during seismic and thermal excursion

events.

- The ex-cryostat guard pipes, that envelope the divertor/blanket pipes, shall be welded to the cryostat. The ex-cryostat guard pipes, together with their associated bellows and cryostat penetrationcover plates forms the cryostat vacuum barrier.

6.2.2 System specific requirements

- Appropriate design provisions shall be included to limit air in- leakage in the cryostat within an acceptable value to prevent a potential ozone production hazard and to prevent water ice build-up on the thermal shield surface, which impairs emissivity.
- Cryostat temperature shall be maintained at room temperature at the pedestal ring and basement section location by appropriate design during normal operating condition.
- Cryostat top lid centre cover shall be bolted joint with lip-seal vacuum tight joint to facilitate the major in cryostat failure of CS magnet removal provision. Cryostat shall have provision for venting system ports for maintenance purpose.
- Cryostat shall have appropriate support provision for approaching and to carry out the In-Cryostat maintenance.

6.2.3 Structural requirements

- The cryostat top lid as well as bottom plate shall be designed for deflection, the deflection shall be limited to 30mm during the normal operating condition.
- The pedestal ring shall be connected to the Magnet gravity supports and the Vacuum Vessel support mechanism. The pedestal ring shall withstand all the loads that are transferred from the Magnets and the VV.
- The 18 columns, these support the pedestal ring from the pit floor, shall have anchor bolts and connection accessories for connecting to the pedestal columns

flange.

- The cryostat skirt supports shall be designed appropriately to with stand the gravity load and seismic force including rocking effects transmitted from the cryostat itself and in-cryostat components. The skirt support shall also allow the movement of cryostat cylinder in radial direction due to thermal loads during accident events. The cryostat skirt supports shall be connected to the embedded parts in the bioshield.
- The radial support lugs of the cryostat support system shall be welded to the out edge of the horizontal plate and the mating lugs shall be connected to the embedded parts in the bioshield to react to the horizontal movement of cryostat during seismic events.

The loads acting on the Cryostat can be divided into four independent categories:

- Pressure loads: these include the external atmospheric pressure in normal operating conditions and coolant leakage pressure as internal pressure during accident. Internal pressure during pressure test.
- Inertial loads: these are caused by accelerations due to gravity and seismic events.
- Electromagnetic (EM) loads: these are not a strong design driver and act upon nearly all conductive structures during transient events (e.g. plasma disruptions, VDEs, and magnet current fast discharge).
- Thermal loads: these are caused by temperature gradients inside the Cryostat structure caused by coolant leakage, heat flux from magnet and VV supports and thermal shield radiation.

6.3 System Design Description

6.3.1 System, Components, Sub-components

The cryostat is a cylindrical Vacuum Vessel, with its axis vertical, and with a flat bottom head and a tori-spherical top lid. The height of cryostat is 25.15m, while the

maximum diameter of the outer cylindrical part is 25.4m, while the diameter of outer cylindrical part is reduced to 17.4m below the VV divertor ports.

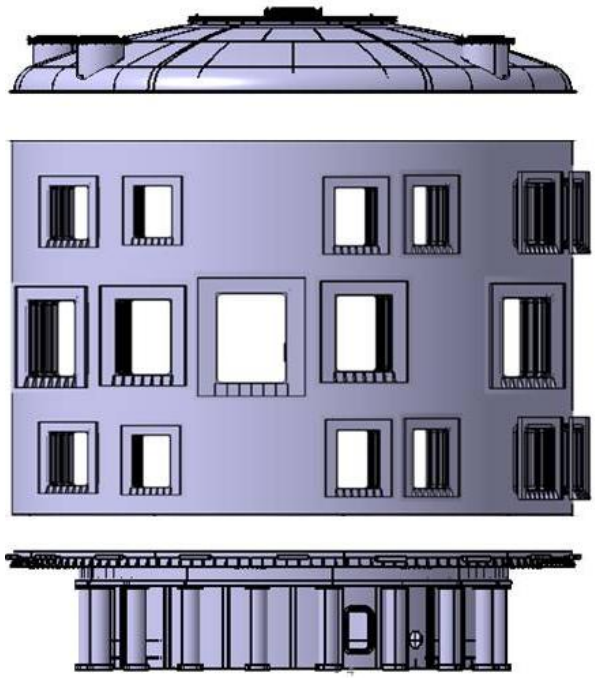

Figure 52 cryostat configuration

The skirt support, which is installed to a stage of the bio-shield wall, supports the upper cryostat. The skirt support allows radial movement of the cryostat shell in case of Helium and water spillage event inside the cryostat.

The horizontal support lugs, with its mating parts embedded in the bio-shield wall, confine the cryostat and the Tokamak basic machine from horizontal movement during seismic events.

The cryostat envelope the Tokamak basic machine, and has penetrations to allow the passage of all the components and systems that are required to operate and maintain the Tokamak and the cryostat.

The port penetrations are connected to VV port ducts and bio-shield port cells by metallic bellows to compensate all relative movements during the normal and off-normal operational regimes and at specified accidental conditions. These bellows system design will also meet relative movements requirements between the as built and operation states.

The cryostat bottom flat head is just above the pit floor level. The cryostat is connected to vacuum pumps and the vacuum monitoring system.

The cryostat has a removable central cover in case of possible removal of CS coils.

The cryostat flat bottom has provision of central welded cover to support initial Tokamak assembly. The cryostat is connected with draining pipe at cryostat bottom to release the water after ICE inside cryostat.

The cryostat is connected with a purging gas pipe to purge the cryostat, when necessary, with nitrogen gas or air. This purging system can also be used to remove decay heat from VV and in-vessel components in certain event scenarios.

The cryostat has all necessary instruments for operation, monitoring and control information.

The cryostat consists of four main sections assembled in the Tokamak pit. These sections are welded in the pit to form the full cryostat. Due to the oversize for road transport to CFTER site, the 4 sections will be fabricated from the segments in the site fabrication workshop before they are assembled in the Tokamak pit.

Cryostat support structure system meets the following functional requirements:

- To sustain vertical loads (gravity and seismic forces including rocking effects) transmitted from the cryostat itself and in-cryostat components.
- To transmit horizontal seismic forces of the Tokamak and the cryostat itself to the building.
- To accommodate thermal movement of the cryostat shell.
- To provide air flow passage inside the cryostat space room during operations.

6.3.2 Cryostat Operation

The main function of the cryostat is to provide a vacuum environment to limit the gas conduction heat loads to the superconducting magnet system during operation. For this function, the cryostat vessel itself is a rather passive system and has no special active control system. The cryostat vacuum pumping system and vacuum leak detection

system will control the vacuum environment inside the cryostat, including the leak detection.

The cryostat and Tokamak start-up schedule shall be:

- Rough pump the cryostat and dehydrate by purging and venting with dry gas.
- High vacuum pump the cryostat to a pressure of 10-4 Pa.
- Cool the thermal shields to liquid nitrogen temperature and magnets to liquid helium temperature.
- Heating system (feedback controlled) starts operation to keep the pedestal ring above 0 ℃.
- Cryostat instrumentation system monitors and records the cryostat operation data.

The states of cryostat during different conditions are listed in Table 29:

Table 29 cryostat working state

CFTER Operation State	Construction/Long Term Maintenance	Short Term Maintenance	Test & Conditioning State	Short Term Stand-by	Plasma Operation
Duration	>30 days	1-30 days		<8 hrs	
Cryostat Pressure	Atmosphere / Vacuum	Vacuum	Vacuum	Vacuum	Vacuum

6.3.3 Interfaces

Cryostat is supported by the building with 18 support columns and skirt support. The weight of Tokamak machine is taken by the cryostat pedestal ring and transferred to building via 18 support columns. The relative movements between cryostat and building are compensated by bellows.

The magnet gravity supports are installed on the pedestal ring. Cryostat also provides penetrations and partial supports for magnet feeders.

The VV supports are installed on the pedestal ring. Cryostat provides ports and

penetration for VV and in-vessel coils. The relative movements between VV ports and cryostat are compensated by port duct bellows.

Cryostat provides supports for lower cryostat thermal shield.

Cryostat provides penetrations to cooling water pipes for cooling of VV, blanket and divertor.

Cryostat provides penetrations to other CFTER systems such as diagnostics, fueling, vacuum pumping, and cryogenic distribution.

Cryostat also provides supports within cryostat for rails and trolleys to perform in-cryostat maintenance.

6.3.4 Maintenance operation

The most probable corrective maintenance for the cryostat is to repair leaks. If the detected helium or air leakage is below the allowable leak rate, the plant will continue operation, and the source of the leakage will be located if possible. During the next scheduled plant outage the leak will be located and repaired. If the leakage exceeds the allowable limits, the plant will be stopped and the leak will be repaired.

The most probable leak sources are the seals of the flange joints, the valves and the penetration bellows. Some of these components are provided with pumped interspaces so that the leak rate can be measured during operation, and leaks mitigated by differential pumping. Hence the leakage from these components will be revealed and located during operation. Other leak sources from the vessels themselves and in-cryostat components, such as cryogenic helium lines and thermal shield helium lines, can be sustained up to the limit of the cryostat helium pumping system, and will be localized and repaired during planned plant outage.

6.4 Conceptual Design Description

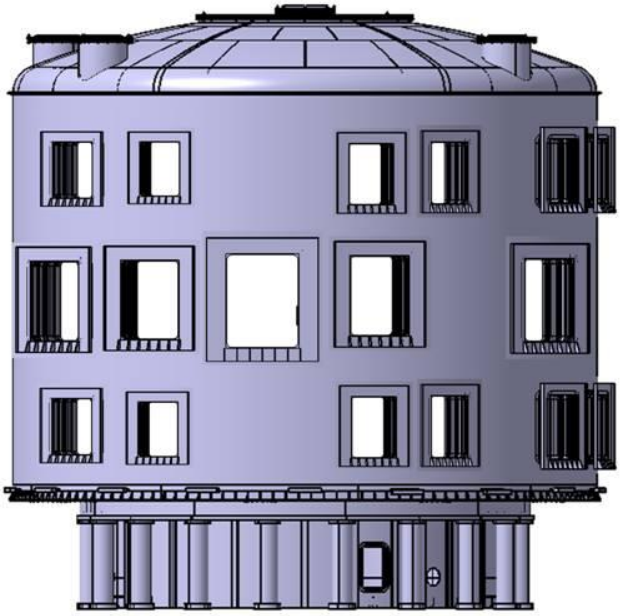

Figure 53 CFETR cryostat overview

The main components that form the full cryostat system are cryostat base section, lower cylinder, upper cylinder, top lid, port duct bellow assembly, port cell bellow assembly, cryostat penetrations, pedestal support columns, cryostat venting system and instrumentation.

6.4.1 Base Section

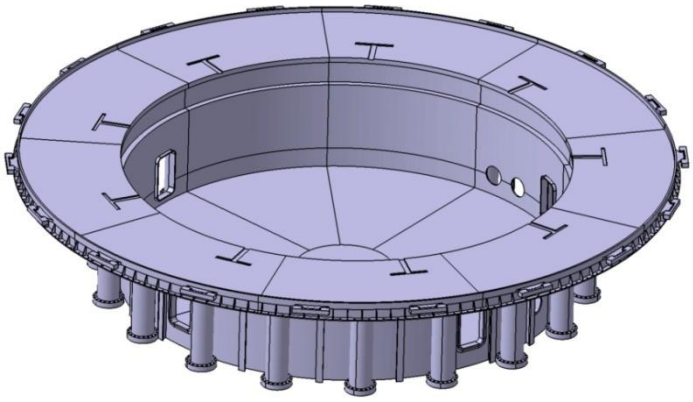

Figure 54 cryostat base section

The cryostat base section consist of flat bottom with sandwiched structure, small cylinder of out diameter, pedestal ring that supports the magnets and vacuum vessel, pedestal columns that support the pedestal ring from the pit floor, horizontal ring and skirt support that support cryostat at the outer region both vertically and toroidally. There is a central cover at the center of bottom plate that is open during construction for the support of TF coils/VV sectors at the center. There are ports and penetrations both on small cylinder and horizontal plate for access, magnet feeders, cooling water pipes, VV drainage pipes, cryostat drainage pipe and instrumentation etc.

There are supporting pads on the bottom head for lower cryostat thermal shield (CTS), while the base section will be welded with lower cylinder in Tokamak pit. The cryostat pedestal ring is required to transfer all loads from the Tokamak vacuum vessel, and the TF and PF coils to the support columns. These loads include the dead weight, seismic forces, reaction forces due to the thermal displacement of the machine and electromagnetic forces. The magnet and VV supports are tied with bolts to the pedestal ring. The pedestal ring structure consists of two cylindrical concentric shells and is supported by 18 support columns connected to the basemat.

The cryostat skirt support is designed to have enough strength to support the weight and seismic load of the upper cryostat including the cylinder, top lid. The skirt support allows radial movement due to thermal deformation of cryostat. This skirt support is an extension of the cryostat cylindrical shell, which is connected in the pit to the bioshield floor by clamps and anchor bolts.

There are 18 horizontal lugs at the outside of skirt to confine the cryostat from horizontal movement during seismic events and to allow radial movement when the cryostat is cooled down under off-normal conditions.

6.4.2 Cylinder

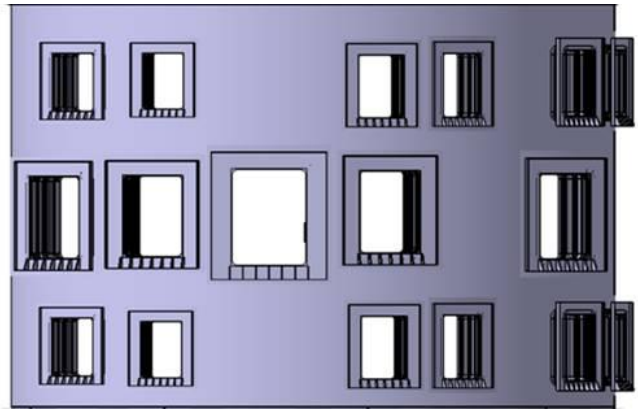

Figure 55cryostat cylinder

The cryostat cylinder is 28.6 m outside diameter and 19 m high. The cylinder is reinforced by toroidal and vertical ribs at the inner side. There are ports and penetrations at 4 levels for VV access, cryostat access, magnet feeders, cooling water pipes, thermal shield coolant pipes, diagnostics, VV pumping, cryostat pumping and instrumentations etc. There are pads and holes on the inner side of cylinder for the supporting of maintenance rails.

6.4.3 Top Lid

The cryostat top lid has a tori-spherical head and reinforced by radial and toroidal ribs. The top lid has a central opening for the removal of CS coils and other openings for maintenance access. There are supporting points at the ribs for maintenance rails and upper CTS.

The top lid will be connected to the upper cylinder by bolting at flanges. Therefore the top lid can be opened when necessary to replace the large components inside cryostat.

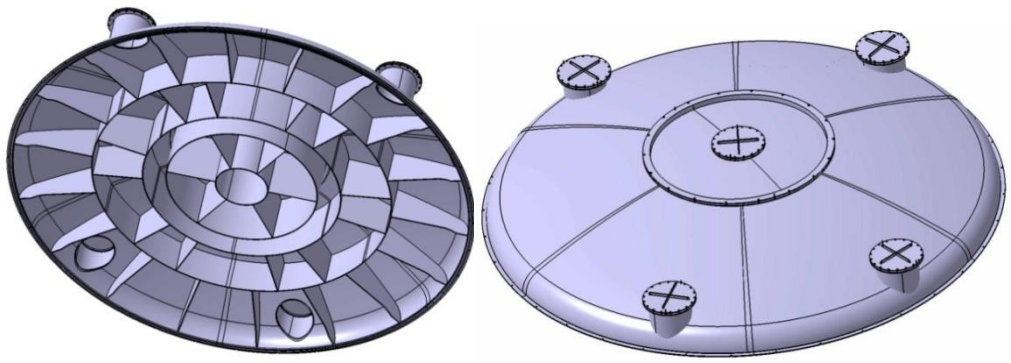

Figure 56 cryostat top lid

6.4.4 Port Duct and Port Cell Bellows

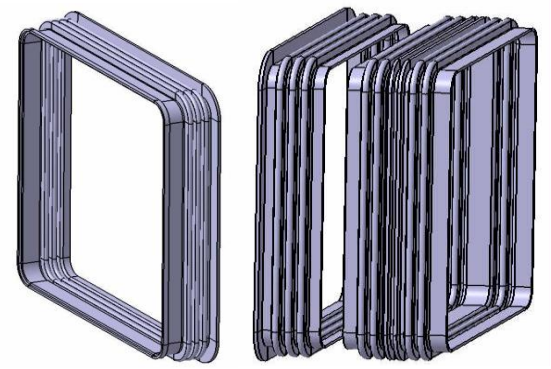

Figure 57 port duct and bellows

Rectangular port duct bellows connecting VV port extensions to cryostat ports at lower, equatorial and upper levels to compensate the relative movements between VV port extensions and cryostat during Tokamak operation and accidents.

Rectangular port cell bellows connecting port cells to cryostat ports at lower, equatorial and upper levels to compensate the relative movements between port cells and cryostat during Tokamak operation and accidents.

6.4.5 Torus Cryo-pump Housing

The cryostat system includes the torus cryo-pump housing (TCPH) which encloses the

torus cryo-pump. The torus cryo-pump is attached to the housing by bolted connection with double metal seals to provide the primary vacuum and tritium confinement sealing. The inter-space between the seals is controlled by service vacuum system.

Generally, the TCPH has the following functions:

- Support the torus cryo-pumps.
- Connect the cryo-pumps to the torus vacuum.
- Provide volume for cryo-pump regeneration.
- Provide tritium confinement and primary vacuum boundary.
- Provides RH docking compatibility for removal of cryo-pump.

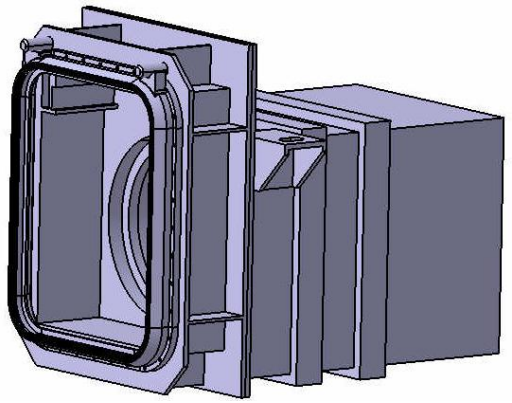

Figure 58 torus cryopump housing

6.5 Summary

In this report, system description of CFETR cryostat is given which has defined the basic functions and basic configurations, then the system design requirements have specified detailed requirements during conceptual design phase, after that general description of system design is described followed by conceptual design description in which main components of cryostat have a conceptual design description with a series of explanations including picture captions.

Simultaneously, conceptual design of magnet system and VV are undergone which will cause corresponding modifications occurring on design of cryostat, including support

suture, penetrations and port cell design etc. Therefore, system design of CFETR cryostat still needs considerable changes along with the evolution of magnet system and VV.

7 Acknowledgements

The conceptual design work of the CFETR tokamak machine covers the great contribution of the whole CFETR group, including:

Team Leader: Songtao Wu, Qiang Li, Yong Liu, Jiangang Li, Yuanxi Wan

Team Member: Yuntao Song, Bingjia Xiao, Sumei Liu, Xufeng Liu, WeiweiXu, Shuangsong Du, Jianghua Wei, Mingxuan Lu, Zhongwei Wang, ZhengpingLuo, JunchuanHao, JinxingZheng, Mingzhun Lei, Songke Wang, Jun Li, Jie Yu, Han Xie, Yonghua Chen, LimanBao, Kun Lu, Yong Cheng, GuangShen, Tingzhi Zhou

Consultant: Yuanxi Wan, DamingGao, PeideWeng, Weiyue Wu, Mingyou Ye

8 Reference

[1] M. Onozuka, K. Ioki, G. Johnson, T. Kodama, G. Sannazzaro, Y. Utin, Design and analysis of the vacuum vessel for RTO/RC-ITER, Fusion Engineering and Design 51-52 (2000) 249-255

[2] Yu. Utin, V. Chuyanov, F.Elio, K. Ioki, L. Jones, V. Komarov, et al, Design progress of the ITER vacuum vessel and ports, Fusion Engineering and Design 75-79 (2005) 571-575

[3] M. Cavinato, A. Portone, G. Saibene, R. Sartori, R. Albanese, G. Ambrosino, et al, Assessment of alternative vessel and blanket design on ITER operation, Fusion Engineering and Design 85 (2010) 2245-2250

[4] K. Ioki, G. Johnson, K. Shimizu, D. Williamson, Design of the ITER vacuum vessel, Fusion Engineering and Design 27 (1995) 39-51

[5] K. Koizumi, M. Nakahira, Y. Itou, E. Tada, G. Johnson, K. Ioki, et al, Design and development of the ITER vacuum vessel, Fusion Engineering and Design 41 (1998) 299-304

[6] K. Ioki, V. Barabash, A. Cardella, F. Elio, Y. Gohar, G. Janeschitz, et al, Design and material selection for ITER first wall/blanket, divertor and vacuum vessel, Journal of Nuclear Materials 258-263 (1998) 74-84

[7] G. Sannazzaro, P. Barabaschi, F. Elio, K. Ioki, N. Miki, M. Onozuka, et al, Critical issues of the structural integrity of the ITER-FEAT vacuum vessel, Fusion Engineering and Design 58-59 (2001) 863-867

[8] M. Onozuka, K. Ioki, G. Sannazzaro, Y. Utin, H. Yoshimura, Design and thermal/hydraulic characteristics of the ITER-FEAT vacuum vessel, Fusion Engineering and Design 58-59 (2001) 857-861

[9] Yu. Utin, K. Ioki, A. Alekeev, Ch. Bachmann, S. Cho, V. Chuyanov, et al, Design progress of the ITER vacuum vessel sectors and port structures, Fusion Engineering and Design 82 (2007) 2040-204